Thesis for the degree of Licentiate of Engineering

Three-nucleon forces in nuclear physics simulations

Tor Djärv

CHALMERS
UNIVERSITY OF TECHNOLOGY

Department of Physics
Chalmers University of Technology
Gothenburg, Sweden 2019

Three-nucleon forces in nuclear

physics simulations

Tor Djärv

Department of Physics
Chalmers University of Technology
SE-412 96 Gothenburg
Sweden
Telephone +46 (0)31-7721000

Cover: Density of the $n = 1$, $l = 2, m = 1$ harmonic-oscillator wavefunctions used for the no-core-shell-model (NCSM)-basis, see chapter 2. The image is produced with a c++ code written by the author.

Chalmers Reproservice
Gothenburg, Sweden 2019

Three-nucleon forces in nuclear

physics simulations

Tor Djärv
Department of Physics
Chalmers University of Technology

Abstract

The aim of this licentiate thesis is to evaluate the normal-ordered two-body (NO2B)-approximation as a computationally promising way to incorporate realistic three-nucleon forces (3NFs) in nuclear many-body simulations using the no-core-shell-model. The existence and importance of 3NFs is predicted in chiral effective field theories of the strong-nuclear force. However, the inclusion of 3NFs renders simulations computationally demanding and this severely limits the size of nuclei that can be studied. Clearly, approximation schemes are needed. In the specific version of the NO2B-approximation that is studied here, the 3NF is normal-ordered with respect to a single Slater-determinant reference state constructed from harmonic-oscillator states, yielding an expansion with zero-, one-, two- and three-nucleon terms. The irreducible three-nucleon part of the original 3NF is assumed to be small and therefore discarded, thus leaving an effective two-nucleon potential. It is found that the predicted ground-state energy of ^{4}He in the NO2B-approximation depends strongly on the choice of many-body basis. The NO2B-approximation breaks the translational symmetry of the Hamiltonian and therefore introduces strong center-of-mass (CM)-mixing in the ^{4}He ground-state. This CM-mixing is shown to be an important reason for the observed basis dependence. Thus, the NO2B approximation is most likely more useful for studies of heavier nuclei. Indeed, the approximation error for the ground-state energy of ^{16}O is observed to be smaller and the results exhibit a weaker dependence on the choice of many-body basis. Finally, it is recommended that CM mixing should be used as a diagnostic to assess the reliability of the NO2B approximation.

Keywords: nuclear physics, three-nucleon forces, normal ordering, configuration interaction, many-body physics

Contents

Chapter 1

Introduction

One of the great scientific milestones of the 20:th century was the discovery of the atomic nucleus in 1913 [1]. Later, it was found that the nucleus consists of protons and neutrons. Since only two fundamental forces, gravity and electromagnetism, were known at the time, it was not understood how the nucleus could hold together. The electrically charged protons repel each other, which would rip the atomic nucleus apart, and gravity is too weak to counteract this repulsion and keep the nucleus together. Therefore, a new fundamental force was needed; one that is strong enough to overcome the electromagnetic repulsion but short ranged enough to not be observable outside the nucleus. In addition, the previous observation of β-decay in 1899 posed another problem. β^--decay changes neutrons into protons while emitting electrons and antineutrinos, and β^+-decay changes protons into neutrons while emitting positrons and neutrinos, called β^+. Neither the electromagnetic force nor gravity can turn protons into neutrons or vice versa. Therefore, the discovery of β-decay too called for a new force. These two new forces were named the strong nuclear force and the weak nuclear force.

Currently, the Standard Model of particle physics is the best known theory for the strong nuclear force, the weak nuclear force and the electromagnetic force, but not gravity. In the standard model, the strong nuclear force is described by quantum-chromodynamics (QCD), where quarks form tightly bound composite particles, such as protons and neutrons, held together by gauge-bosons, called gluons. The weak nuclear force is mediated by $W^{\pm}$- and Z-bosons between quarks and leptons (electron like particles and neutrinos) [2].

Despite the tremendous success of the Standard Model when it comes to describing and predicting high-energy phenomena, the low-energy regime of the strong and weak nuclear forces are still not well understood. It is currently not clear how atomic

nuclei are formed from a theory of interacting quarks and gluons. Computing nuclear observables directly from QCD can in principle be done via the lattice-QCD-method [3]. However, this approach is extremely computationally demanding, yielding unphysical results, and is currently only applicable for the lightest nuclei. The weak nuclear force is also not well understood, one example is the neutron half-life anomaly, i.e the observation that the neutron half-life, when measured in different ways gives different results [4]. For the rest of this work I will, only focus on the strong nuclear force.

QCD is non-perturbative at the low energies relevant to nuclear physics. To handle this problem, one can introduce effective-field-theories (EFTs) [5, 6, 7]. An EFT is a general description of a physical system in terms of some relevant degrees of freedom, that repsects some underlying symmetries [5]. An EFT description introduces new parameters that must be determined from data so that it reproduces the physics of the system. A commonly used class of EFTs is the chiral-effective-field-theories (χEFTs). The degrees of freedom of the χEFTs are no longer quarks and gluons, instead it is expressed with heavier particles, such as protons, neutrons and pions, that are more relevant for the low momentum scale at which nuclei reside [6, 7].

Although χEFTs can be used to derive a description of the strong inter-nucleon interaction, one still needs to solve the many-body Schrödinger equation (MBSE). There are many computational methods to solve the MBSE [8, 9, 10, 11]. One such method is the NCSM [8], where the full nuclear Hamiltonian is expressed in a finite dimensional many-body basis, turning the MBSE to a finite matrix-eigenvalue problem that can be solved numerically. The NCSM-basis is often constructed from a harmonic-oscillator (HO)-basis. A more exhaustive presentation of the NCSM used in this work can be found in chapter 2.

Employing χEFT-derived potentials in the NCSM method, and other methods, is no trivial matter. χEFTs predict the existence of many-nucleon forces that can not be ignored [6, 7]. The number of non-zero matrix-elements in the Hamiltonian increases roughly exponentially with the number of particles interacting via the many-body force. For this reason, the first nuclear simulations with chiral interactions were limited to only involve two-nucleon forces (2NFs). Full three-nucleon forces (3NFs) have been included only in the last two decades [9, 12, 13].

Although it is straightforward to algebraically include 3NFs, and other many-nucleon forces, in the NCSM, the computational complexity is huge and severely limits which atomic nuclei that can be studied with them. To remedy the situation an approximation scheme is needed. One such scheme is the normal-ordering-two-body (NO2B)-approximation [14], which can also be used in other many-body methods

than the NCSM. In the NO2B-approximation the 3NF potential is normal ordered relative some many-body state, called the reference state, yielding an expansion of three-, two-, one- and zero-body potentials. This expansion is an exact representation of the 3NF and is not an approximation. However, the remaining three-body potential is approximated to have a small contribution to the ground-state energy compared to the other potentials and can therefore be discarded [14].

The reference state of the NO2B-approximation can be chosen in many ways. It is common to choose a single Slater determinant as the reference state, this is called the single-reference-normal-ordering-two-body (SR-NO2B)-approximation [14]. However, a general many-body state, composed of many Slater determinants, can also be chosen which is called the multi-reference-normal-ordering-two-body (MR-NO2B)-approximation [15]. In this work I explore a version of the SR-NO2B-approximation where the Slater determinant is constructed from the same HO-eigenstates as the NCSM-basis. Throughout this work the term NO2B will be used to mean this particular version of SR-NO2B unless something else is explicitly stated. The NO2B-approximation used in this work is described in more detail in chapter 3.

Introducing an approximation comes with some cost. It is therefore the specific aim of this work to explore some consequences of the NO2B-approximation. First, the NO2B-approximation breaks the translational invariance of the 3NF. This is because the reference state is only a Slater determinant in one frame of reference, and must be constructed from multiple ones in all other frames. Since the NO2B procedure breaks the translational symmetry of the interaction, an exact separation with respect to Center-of-Mass (CM)- and intrinsic excitaitons is no longer guaranteed and CM-mixing must be expected in the resulting description of nuclear ground states. This CM-problem is discussed in detail in chapter 4 where I also discuss two metrics to quantify the level of CM-mixing.

Physical observables should not depend on the choice of many-body basis. However, the HO Slater determinant used as reference state in this version of the NO2B-approximation depends strongly on the HO-frequency of the NCSM-basis. Since, the NO2B-potential inherit the frequency dependence from the reference state it is not guaranteed that observables are independent of the basis any more. In chapter 5 this basis dependence is explored, and a connection to the CM-mixing problem is investigated.

In chapter 6, I discuss the consequences of the results in chapter 5, for the SR-NO2B-approximation in a HO-basis. I also suggest, as a best practice, to always quantify the amount of CM-mixing when using the NO2B-approximation.

Chapter 2

Solving the many-body Schrödinger equation

In this work I aim to study the effect of 3NFs in light atomic nuclei. To do this the internal dynamics of the atomic nucleus must be determined, which is governed by the many-body-Schrödinger-equation (MBSE)

$$\hat{H}\,|\Psi\rangle = E\,|\Psi\rangle\,. \tag{2.1}$$

In this work the Hamiltonian includes up to three-nucleon forces,

$$\hat{H} = \hat{T}_{\text{int}} + \hat{V}_{\text{2NF}} + \hat{V}_{\text{3NF}}, \tag{2.2}$$

where $\hat{T}_{\text{int}}$ is the intrinsic kinetic energy, $\hat{V}_{\text{2NF}}$ and $\hat{V}_{\text{3NF}}$ are the 2NFs and 3NFs, that depend only on intrinsic coordinates. In particular there is no dependence on the CM-coordinates.

To solve the MBSE I use the NCSM [16]. This chapter intends to describe this many-body method, present some useful properties and finally discuss the problem with increased computational complexity introduced by 3NFs.

2.1 The No Core Shell Model

The way the NCSM solves the MBSE is in principle quite simple. The MBSE is expanded in a finite dimensional many-body basis

$$\{|\Phi_i\rangle\}_{i=1}^{D}, \tag{2.3}$$

where D is the dimension. In this basis the MBSE becomes a finite matrix eigenvalue problem

$$\sum_{j=1}^{D} \langle \Phi_i | \hat{H} | \Phi_j \rangle \, c_j = E c_i. \tag{2.4}$$

The coefficients c_i are the amplitudes in the expansion of the eigenstate

$$\left| \Psi^{\mathrm{NCSM}} \right\rangle = \sum_{i=1}^{D} c_i \left| \Phi_i \right\rangle . \tag{2.5}$$

The matrix eigenvalue problem in equation (2.4) can be solved numerically. With increasing dimension, the size of the matrix becomes so large that iterative algorithms such as Lanczos are preferred.

The distinguishing feature of the NCSM is the choice of the total-energy-truncated many-body HO-basis. In particular, the states $|\Phi_i\rangle$ are chosen to be antisymmeterized eigenstates to the Hamiltonian

$$\hat{H}_{\mathrm{HO}} = \sum_{i=1}^{A} \left(\frac{\hat{p}_i^2}{2m} + \frac{m\omega^2}{2} \hat{r}_i^2 \right), \tag{2.6}$$

with frequency $\hbar\omega$ and where $\hat{p}_i$ and $\hat{r}_i$ are the momentum and position of nucleon i in three-dimensions. In addition to the HO-states, the states are also equipped with spin and isospin quantum numbers. Due to the symmetries of $\hat{H}_{\mathrm{HO}}$ it is possible to either use relative (Jacobi)-coordinates or lab-coordinates. In this work I choose the latter since the basis states become easier to antisymmeterize. The single-particle degrees of freedom are spanned by states on the form

$$|\alpha\rangle = |n, l, j, m, t_z\rangle . \tag{2.7}$$

The antisymmetrization, due to the fermionic nature of the nucleons, is, in this work, imposed by requiring that the many-body states are Slater-determinants of the single-nucleon states in equation (2.7),

$$|\Phi_i\rangle = \frac{1}{\sqrt{A!}} \begin{vmatrix} |\alpha_{i,1}\rangle_1 & |\alpha_{i,1}\rangle_2 & \cdots & |\alpha_{i,1}\rangle_A \\ |\alpha_{i,2}\rangle_1 & |\alpha_{i,2}\rangle_2 & \cdots & |\alpha_{i,2}\rangle_A \\ \vdots & \vdots & \ddots & \vdots \\ |\alpha_{i,A}\rangle_1 & |\alpha_{i,A}\rangle_2 & \cdots & |\alpha_{i,A}\rangle_A \end{vmatrix} = \prod_{j=1}^{A} \hat{c}^{\dagger}_{\alpha_{i,j}} |\rangle , \tag{2.8}$$

where $\hat{c}^{\dagger}_{\alpha}$ is a second-quantization fermionic creation operator.

In practice, the many-body basis must be truncated. In the NCSM, the total number of HO-excitations above the A-fermionic HO-ground state is limited, yielding the inequality

$$\sum_{j=1}^{A}(2n_{i,j} + l_{i,j}) - N_{\min} \leq N_{\max}. \tag{2.9}$$

$N_{\min}$ is obtained by filling the Z lowest proton states and the $A - Z$ lowest neutron states. This is illustrated in figure 2.1 where the minimal configuration for ^{16}O is shown.

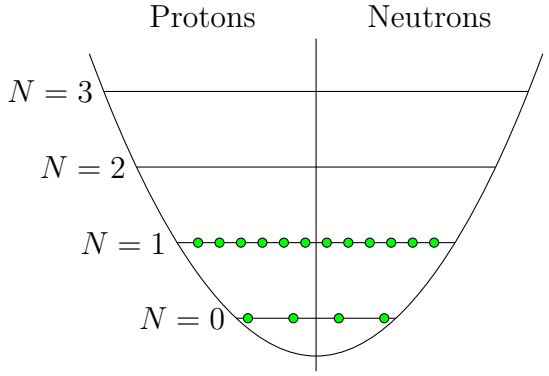

Figure 2.1: The lowest possible HO-configuration for ^{16}O. Here $N = 2n + l$ is the single nucleon HO-energy excitation. In this case $N_{\min} = 12$ since there are 12 nucleons in the first excited HO-shell.

$N_{\max}$ in inequality (2.9) is the NCSM-truncation parameter. The NCSM is a variational method in $N_{\max}$ and thus fulfils that $E_{\text{gs}}^{\text{NCSM}} \geq E_{\text{gs}}$ for $N_{\max} < \infty$, where E_{gs} is the ground-state energy in the untruncated Hilbert-space. This is visualized in figure 2.2 where the ground-state energy of ^{4}He is computed with NCSM using the 2NF-part of the NNLO-sat interaction [17]. The NCSM-basis frequency $\hbar\omega$ is set to 20 MeV for this calculation.

The curve traced out by $E_{\text{gs}}^{\text{NCSM}}$ as a function of $N_{\max}$ in figure 2.2 is close to be a shifted exponential of the form $E_{\text{gs}}^{\text{NCSM}} \approx E_{\text{gs}} + ae^{-bN_{\max}}$. It is therefore common to extrapolate NCSM results using such function [18, 19, 20]. However, recently more sophisticated methods for extrapolation have been developed. A more accurate extrapolation technique exploits the similarity between the NCSM-basis and that of a hyper-spherical infinite well with an IR cutoff radius. The ground-state energy is then desribed by $E_{\text{gs}}^{\text{NCSM}} \approx E_{\text{gs}} + ae^{-bL_{\text{eff}}}$ where L_{eff} is the IR-length scale [21].

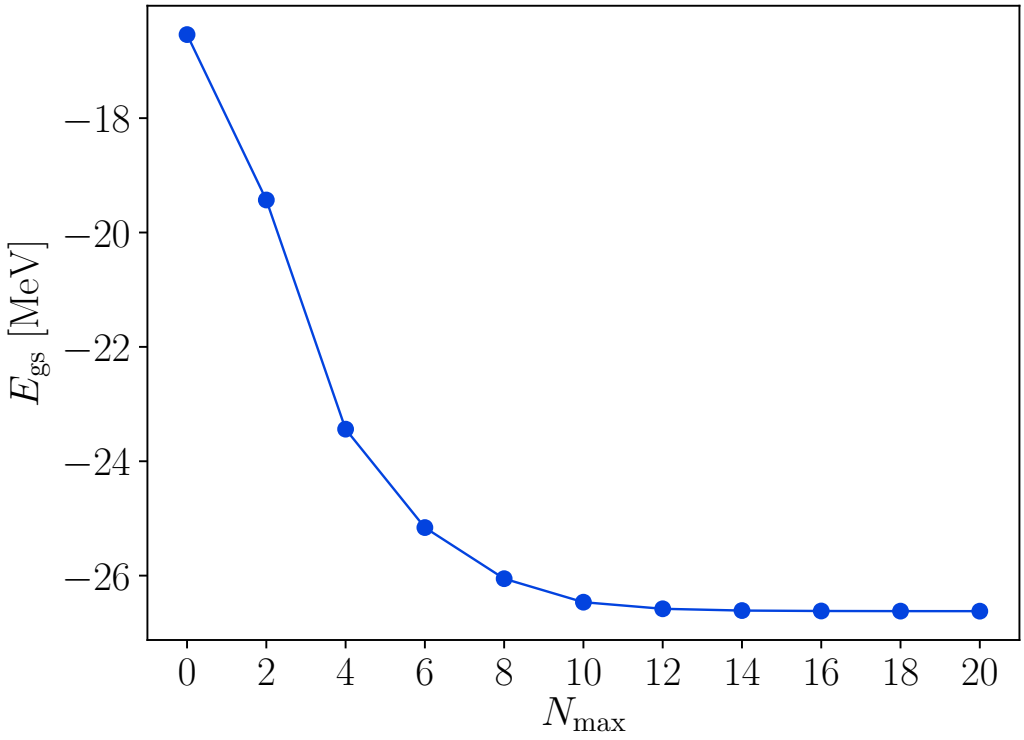

Figure 2.2: The ground-state energy of ^{4}He computed with NCSM for $\hbar\omega = 20$ in increasing model space with a 2NF interaction based on NNLO-sat [17]. The results illustrate the variational nature of NCSM.

2.2 Three-nucleon forces in the No Core Shell Model

3NFs are fairly straight-forward to implement in the NCSM. The same theoretical framework as for 2NFs can be used to treat 3NFs. The technical details of implementing 3NFs in NCSM is, however, not relevant for the further discussion.

There is, however, a problem with implementing 3NFs in NCSM that deserves to be mentioned. That is the increase in number of non-zero matrix-element (NZME) compared to 2NFs. This makes simulations with 3NFs orders of magnitude more computationally heavy than with only 2NFs. In figure 2.3 this is illustrated by plotting the number of NZME of V_{3NF} and V_{2NF} in an ^{16}O NCSM-basis. The number of NZME are approximate estimates where $\#\mathrm{NZME(3NF)} = D^{3/2}$ and $\#\mathrm{NZME(2NF)} = D^{5/4}$ [22, 23], and therefore not computed directly from the method. On the left axis is the number of NZME, the bottom axis is the NCSM-basis dimension, the top axis is

$N_{\max}$ and on the right axis is the required memory space needed to explicitly store the matrices as double precision IEEE floating-point numbers. Note the logarithmic scale on three of the axes.

It is clear in figure 2.3 that the number of NZME of the 3NFs increase much faster with increasing truncation $N_{\max}$ compared to the 2NFs. For instance, at $N_{\max} = 2$ there are about 6 times more 3NF than 2NF elements and at $N_{\max} = 4$ there are 22 times as many 3NF than 2NF elements.

With the NCSM code pAntoine [24], a parallelized version of Antoine [25] I am able to compute the ^{16}O ground-state energy with only 2NF up to $N_{\max} = 8$. If the Hamiltonian was to be stored explicitly, which it is not, it would take roughly 680 GB of memory. If 3NFs would be included the Hamiltonian would require 157 times more memory, roughly 107 TB. The calculation with pAntoine for ^{16}O and only 2NF takes roughly 8 hours to perform on one node with a 32 core Intel Xeon Gold 6130 processor and 96 GB of RAM. Note that pAntoine uses the Lanczos algorithm to diagonalize the Hamiltonian, where matrix-vector multiplications are repeatedly performed. The time complexity of a matrix-vector multiplication is linear in the number of NZME. Assuming that the same number of Lanczos iterations are needed it would take approximately 2 months to do the same calculation with the inclusion of 3NF. Furthermore, the ground-state energy for ^{16}O computed with NCSM is far from fully converged at $N_{\max} = 8$. It is thus clear that including 3NF in NCSM severely limits the size of the nuclei that can be studied.

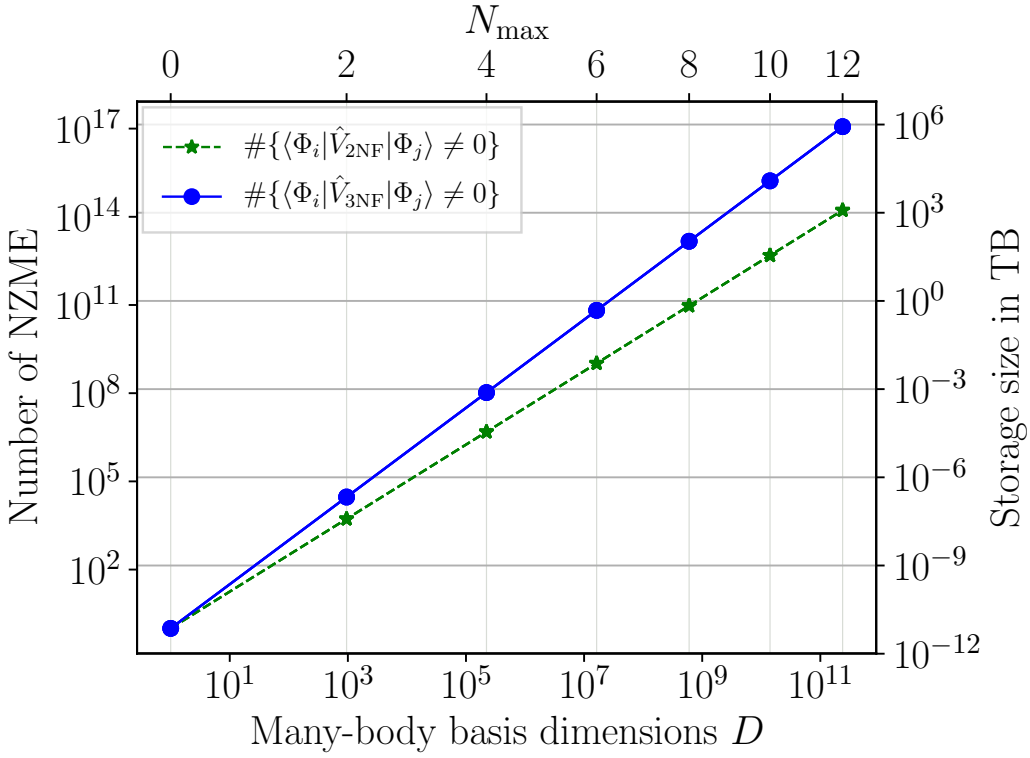

Figure 2.3: The number of non-trivial zero matrix elements of 2NFs (green dashed line) and 3NFs (blue solid line) for the ^{16}O system.

Chapter 3

The Normal-Ordering approximation

I discussed the need for 3NFs in chapter 1, where I pressented the theoretical motivation for them in *ab initio* nuclear physics. In section 2.2 I discussed the additional computational complexity by including 3NFs in the NCSM and how it severely limits the size of nuclei that can be studied. These two facts, the need for 3NFs and the computational complexity they cause, is a dilemma that needs to be solved. In this chapter I present a possible solution, the SR-NO2B-approximation [14]. The SR-NO2B-approximation, approximates the 3NF as an effective 2NF and thus incorporates some physics from 3NFs at the computational cost of 2NFs. This is done by normal ordering the 3NF relative a single Slater determinant, yielding an expansion of three-, two-, one- and zero-body terms. If the reference state is similar to the ground state the contribution of the remaining three-body term will be small and can thus be discarded. The normal-ordering procedure is explained in more detail in section 3.1. In section 3.2 I discuss the limitation to closed-core nuclei. Section 3.3 presents a ^{4}He benchmark of the NO2B approximation. The last section, 3.4, discusses the C-code, cNO2B, that implements the NO2B-approximation and is a product of this work.

3.1 Derivation of the approximation

The NO2B approximation approximates a 3NF,

$$\hat{V}_{\text{3NF}} = \frac{1}{36} \sum_{\substack{\alpha,\beta,\gamma \\ \alpha',\beta',\gamma'}} \langle \alpha,\beta,\gamma | V_{\text{3NF}} | \alpha',\beta',\gamma' \rangle \, \hat{c}^\dagger_\alpha \hat{c}^\dagger_\beta \hat{c}^\dagger_\gamma \hat{c}_{\gamma'} \hat{c}_{\beta'} \hat{c}_{\alpha'} \tag{3.1}$$

as an effective 2NF,

$$\hat{V}_{\mathrm{3NF}}^{NO2B} = \frac{1}{4} \sum_{\substack{\alpha,\beta \\ \alpha',\beta'}} \langle \alpha, \beta | V_{\mathrm{3NF}}^{NO2B} | \alpha', \beta' \rangle \, \hat{c}_{\alpha}^{\dagger} \hat{c}_{\beta}^{\dagger} \hat{c}_{\beta'} \hat{c}_{\alpha'}, \tag{3.2}$$

where $\hat{c}_{\alpha}^{\dagger}$ and $\hat{c}_{\alpha}$ are second-quatization creation and annihilation operators. This is achieved by normal-ordering the 3NF in equation (3.1) relative a single Slater determinant,

$$|\Psi_{\mathrm{ref}}\rangle = \hat{c}_{\alpha_1}^{\dagger} \hat{c}_{\alpha_2}^{\dagger} \cdots \hat{c}_{\alpha_A}^{\dagger} |\rangle \,, \quad R = \{\alpha_1, \ldots, \alpha_A\} \tag{3.3}$$

where $|\rangle$ is the vacuum state and R will be referred to as the reference set. It is possible to generalize this method to reference states that cannot be written as a single Slater determinant, this is called multi-reference normal-ordering [15]. However, this generalization will not be covered in this work.

3.1.1 The normal-ordering expansion

I will apply Wick's theorem [26] to do the normal ordering of the 3NF in equation (3.1). However, before I can do that I have to define what is meant by normal ordering, and I have to introduce the concept of Wick contractions of two second-quantization operators.

In this work I notate a normal-ordered product, relative $|\Psi_{\mathrm{ref}}\rangle$, as $\left\{\hat{c}_{\alpha}^{\dagger} \hat{c}_{\beta}^{\dagger} \hat{c}_{\gamma}^{\dagger} \hat{c}_{\gamma'} \hat{c}_{\beta'} \hat{c}_{\alpha'}\right\}$. The normal ordering of a product of creation and annihilation operators, for instance $\hat{c}_{\alpha}^{\dagger} \hat{c}_{\beta}^{\dagger} \hat{c}_{\gamma}^{\dagger} \hat{c}_{\gamma'} \hat{c}_{\beta'} \hat{c}_{\alpha'}$, can now be defined (similarly to the definition by W.H.Dickhoff and Neck [26]) with the two following rules:

- All creation operators $\hat{c}_{\alpha}^{\dagger}$ such that $\alpha \in R$ and all annihilation operators $\hat{c}_{\beta}$ such that $\beta \notin R$ are moved to the right.
- All creation operators $\hat{c}_{\alpha}^{\dagger}$ such that $\alpha \notin R$ and all annihilation operators $\hat{c}_{\beta}$ such that $\beta \in R$ are moved to the left.

These two rules give the property that $\{A\} |\Psi_{\mathrm{ref}}\rangle = 0$ and $\langle \Psi_{\mathrm{ref}}| \{A\} = 0$, where A as an arbitrary product of creation and annihilation operators.

As mentioned before it is also necessary to introduce the Wick contraction of a pair of creation and annihilation operators. Assuming that I have the product $\hat{a}\hat{b}$ where $\hat{a}$ and $\hat{b}$ are creation or annihilation operators then a contraction, $\hat{a}\hat{b}$, is defined as a complex number such that

$$\hat{a}\hat{b} = \hat{a}\hat{b} - \left\{\hat{a}\hat{b}\right\}. \tag{3.4}$$

The value of the contraction can be evaluated by using that the normal-ordered term has a zero expectation value with the reference state and thus I get that

$$\overbracket{\hat{a}\hat{b}} = \langle \Psi_{\text{ref}} | \, \hat{a}\hat{b} \, | \Psi_{\text{ref}} \rangle \,. \tag{3.5}$$

In my case, with a single Slater-determinant as reference state, I can evaluate some specific contractions by exploiting equation (3.5),

$$\overbracket{\hat{c}^{\dagger}_{\alpha}\hat{c}_{\beta}} = \begin{cases} \delta_{\alpha,\beta} & \text{if } \alpha,\beta \in R \\ 0 & \text{otherwise} \end{cases} = \delta_{\alpha,\beta\in R} \tag{3.6}$$

$$\overbracket{\hat{c}_{\alpha}\hat{c}^{\dagger}_{\beta}} = \begin{cases} \delta_{\alpha,\beta} & \text{if } \alpha,\beta \notin R \\ 0 & \text{otherwise} \end{cases} = \delta_{\alpha,\beta\notin R} \tag{3.7}$$

where I have introduced $\delta_{\alpha,\beta\in R}$ and $\delta_{\alpha,\beta\notin R}$ as shorthand notation for the conditional statements. This can be interpreted in the particle-hole formalism: $\hat{c}^{\dagger}_{\alpha}$ for $\alpha \notin R$ creates a particle while $\hat{c}_{\alpha}$ for $\alpha \in R$ creates a hole. Contraction (3.6) is then a contraction between hole creation and annihilation operators, while (3.7) is a contraction between particle creation and annihilation operators.

To rewrite the 3NF in equation (3.1) I apply Wick's theorem [26], which states that a product of creation and annihilation operators can be rewritten as the sum of the normal-ordered product and all possible contractions. In the 3NF I have therefore

$$\begin{aligned} \hat{c}^{\dagger}_{\alpha}\hat{c}^{\dagger}_{\beta}\hat{c}^{\dagger}_{\gamma}\hat{c}_{\gamma'}\hat{c}_{\beta'}\hat{c}_{\alpha'} = & \left\{\hat{c}^{\dagger}_{\alpha}\hat{c}^{\dagger}_{\beta}\hat{c}^{\dagger}_{\gamma}\hat{c}_{\gamma'}\hat{c}_{\beta'}\hat{c}_{\alpha'}\right\} \\ & + \left\{\hat{c}^{\dagger}_{\alpha}\hat{c}^{\dagger}_{\beta}\hat{c}^{\dagger}_{\gamma}\hat{c}_{\gamma'}\hat{c}_{\beta'}\hat{c}_{\alpha'}\right\} + \left\{\hat{c}^{\dagger}_{\alpha}\hat{c}^{\dagger}_{\beta}\hat{c}^{\dagger}_{\gamma}\hat{c}_{\gamma'}\hat{c}_{\beta'}\hat{c}_{\alpha'}\right\} + \left\{\hat{c}^{\dagger}_{\alpha}\hat{c}^{\dagger}_{\beta}\hat{c}^{\dagger}_{\gamma}\hat{c}_{\gamma'}\hat{c}_{\beta'}\hat{c}_{\alpha'}\right\} \\ & + \cdots 6 \text{ more single contractions} \cdots \\ & + \left\{\hat{c}^{\dagger}_{\alpha}\hat{c}^{\dagger}_{\beta}\hat{c}^{\dagger}_{\gamma}\hat{c}_{\gamma'}\hat{c}_{\beta'}\hat{c}_{\alpha'}\right\} + \left\{\hat{c}^{\dagger}_{\alpha}\hat{c}^{\dagger}_{\beta}\hat{c}^{\dagger}_{\gamma}\hat{c}_{\gamma'}\hat{c}_{\beta'}\hat{c}_{\alpha'}\right\} + \left\{\hat{c}^{\dagger}_{\alpha}\hat{c}^{\dagger}_{\beta}\hat{c}^{\dagger}_{\gamma}\hat{c}_{\gamma'}\hat{c}_{\beta'}\hat{c}_{\alpha'}\right\} \\ & + \cdots 15 \text{ more double contractions} \cdots \\ & + \left\{\hat{c}^{\dagger}_{\alpha}\hat{c}^{\dagger}_{\beta}\hat{c}^{\dagger}_{\gamma}\hat{c}_{\gamma'}\hat{c}_{\beta'}\hat{c}_{\alpha'}\right\} + \left\{\hat{c}^{\dagger}_{\alpha}\hat{c}^{\dagger}_{\beta}\hat{c}^{\dagger}_{\gamma}\hat{c}_{\gamma'}\hat{c}_{\beta'}\hat{c}_{\alpha'}\right\} + \left\{\hat{c}^{\dagger}_{\alpha}\hat{c}^{\dagger}_{\beta}\hat{c}^{\dagger}_{\gamma}\hat{c}_{\gamma'}\hat{c}_{\beta'}\hat{c}_{\alpha'}\right\} \\ & + \left\{\hat{c}^{\dagger}_{\alpha}\hat{c}^{\dagger}_{\beta}\hat{c}^{\dagger}_{\gamma}\hat{c}_{\gamma'}\hat{c}_{\beta'}\hat{c}_{\alpha'}\right\} + \left\{\hat{c}^{\dagger}_{\alpha}\hat{c}^{\dagger}_{\beta}\hat{c}^{\dagger}_{\gamma}\hat{c}_{\gamma'}\hat{c}_{\beta'}\hat{c}_{\alpha'}\right\} + \left\{\hat{c}^{\dagger}_{\alpha}\hat{c}^{\dagger}_{\beta}\hat{c}^{\dagger}_{\gamma}\hat{c}_{\gamma'}\hat{c}_{\beta'}\hat{c}_{\alpha'}\right\} . \end{aligned} \tag{3.8}$$

After some algebra the 3NF in equation (3.1) can be written as

$$\begin{aligned}
\hat{V}_{\rm 3NF} =& \overbrace{\frac{1}{36}\sum_{\substack{\alpha,\beta,\gamma\\ \alpha',\beta',\gamma'}} \langle\alpha,\beta,\gamma|V_{\rm 3NF}|\alpha',\beta',\gamma'\rangle \left\{\hat{c}^\dagger_\alpha\hat{c}^\dagger_\beta\hat{c}^\dagger_\gamma\hat{c}_{\gamma'}\hat{c}_{\beta'}\hat{c}_{\alpha'}\right\}}^{\hat{W}^{3b}_{\rm 3NF}} \\
&+ \overbrace{\frac{1}{4}\sum_{\substack{\alpha,\beta,\gamma\\ \alpha',\beta',\gamma'}} \langle\alpha,\beta,\gamma|V_{\rm 3NF}|\alpha',\beta',\gamma'\rangle\, \delta_{\gamma,\gamma'\in R} \left\{\hat{c}^\dagger_\alpha\hat{c}^\dagger_\beta\hat{c}_{\beta'}\hat{c}_{\alpha'}\right\}}^{\hat{W}^{2b}_{\rm 3NF}} \\
&+ \overbrace{\frac{1}{2}\sum_{\substack{\alpha,\beta,\gamma\\ \alpha',\beta',\gamma'}} \langle\alpha,\beta,\gamma|V_{\rm 3NF}|\alpha',\beta',\gamma'\rangle\, \delta_{\beta,\beta'\in R}\delta_{\gamma,\gamma'\in R} \left\{\hat{c}^\dagger_\alpha\hat{c}_{\alpha'}\right\}}^{\hat{W}^{1b}_{\rm 3NF}} \\
&+ \overbrace{\frac{1}{6}\sum_{\substack{\alpha,\beta,\gamma\\ \alpha',\beta',\gamma'}} \langle\alpha,\beta,\gamma|V_{\rm 3NF}|\alpha',\beta',\gamma'\rangle\, \delta_{\alpha,\alpha'\in R}\delta_{\beta,\beta'\in R}\delta_{\gamma,\gamma'\in R}}^{W^{0b}_{\rm 3NF}} .
\end{aligned} \tag{3.9}$$

The normal-ordered products, $\left\{\hat{c}^\dagger_\alpha\hat{c}_{\alpha'}\right\}$, $\left\{\hat{c}^\dagger_\alpha\hat{c}^\dagger_\beta\hat{c}_{\beta'}\hat{c}_{\alpha'}\right\}$, and $\left\{\hat{c}^\dagger_\alpha\hat{c}^\dagger_\beta\hat{c}^\dagger_\gamma\hat{c}_{\gamma'}\hat{c}_{\beta'}\hat{c}_{\alpha'}\right\}$ ensures that at least one-, two- and three-particle-hole exciations can have non-zero expectation values with the one, two and three-body terms. This has the implicit consequence that the sum over the indices connected to these products are only over indices outside the reference state.

3.1.2 Approximating the three-nucleon force

To this point no approximation has been made; the expansion in equation (3.9) is an exact representation of the full 3NF. To introduce the approximation I will consider three cases:

i. the reference state $|\Psi_{\rm ref}\rangle$, is the dominant component of the ground state.

ii. the reference state, and some one-particle one-hole states dominate the ground state.

iii. the reference state, some one-particle one-hole states and some two-particle two-hole states dominate the ground state.

For case i., the ground state can be written as

$$|\Psi_{\text{gs}}\rangle = N\left(|\Psi_{\text{ref}}\rangle + \varepsilon\,|\Psi_{\text{rest}}\rangle\right) \tag{3.10}$$

where $N = \frac{1}{\sqrt{1+\varepsilon^2}}$ is a normalization constant, $\varepsilon > 0$ is much smaller than one and $\langle\Psi_{\text{ref}}|\Psi_{\text{rest}}\rangle = 0$. The ground-state expectation value of the 3NF is

$$\begin{aligned}\langle\Psi_{\text{gs}}|\hat{V}_{\text{3NF}}|\Psi_{\text{gs}}\rangle =& W^{0b}_{\text{3NF}} \\ &+ N^2\varepsilon^2\Big(\langle\Psi_{\text{rest}}|\hat{W}^{3b}_{\text{3NF}}|\Psi_{\text{rest}}\rangle \\ &+ \langle\Psi_{\text{rest}}|\hat{W}^{2b}_{\text{3NF}}|\Psi_{\text{rest}}\rangle \\ &+ \langle\Psi_{\text{rest}}|\hat{W}^{1b}_{\text{3NF}}|\Psi_{\text{rest}}\rangle\Big).\end{aligned} \tag{3.11}$$

The W^{0b}_{3NF} term gets contributions from all parts of $|\Psi_{\text{gs}}\rangle$ which is normalized to one and thus the prefactor is one. The dominant contribution from the 3NF to the ground-state energy comes in this case from the W^{0b}_{3NF} term of the 3NF. The 3NF could therefore be approximated as

$$\hat{V}_{\text{3NF}} \approx W^{0b}_{\text{3NF}} \equiv \hat{V}^{\text{NO0B}}_{\text{3NF}}. \tag{3.12}$$

This will be referred to as the normal-ordering-zero-body (NO0B)-approximation of the 3NF.

In case ii. the ground-state is dominated by contributions from the reference state and one-particle one-hole configurations,

$$|\Psi_{\text{gs}}\rangle = N\left(|\Psi_{\text{ref}}\rangle + c\,|\Psi_{\text{1p-1h}}\rangle + \varepsilon\,|\Psi_{\text{rest}}\rangle\right), \tag{3.13}$$

where $N = \frac{1}{\sqrt{1+|c|^2+\epsilon^2}}$ is the normalization constant,

$$|\Psi_{\text{1p-1h}}\rangle = \sum_{p\notin R, h\in R}\xi_{p,h}\hat{c}^\dagger_p\hat{c}_h\,|\Psi_{\text{ref}}\rangle \tag{3.14}$$

is a normalized sum over one-particle one-hole excitations, $\varepsilon > 0$ is still assumed to be small, and c is a complex number with absolute magnitude of order one. The

ground-state expectation of the 3NF is in this case

$$\begin{aligned}\langle\Psi_{\rm gs}|\hat{V}_{\rm 3NF}|\Psi_{\rm gs}\rangle =& W^{0b}_{\rm 3NF} \\ &+ N^2|c|^2\,\langle\Psi_{\rm 1p-1h}|\hat{W}^{1b}_{\rm 3NF}|\Psi_{\rm 1p-1h}\rangle \\ &+ N^2\varepsilon^2\Big(\,\langle\Psi_{\rm rest}|\hat{W}^{1b}_{\rm 3NF}|\Psi_{\rm rest}\rangle \\ &+\,\langle\Psi_{\rm rest}|\hat{W}^{2b}_{\rm 3NF}|\Psi_{\rm rest}\rangle \\ &+\,\langle\Psi_{\rm rest}|\hat{W}^{3b}_{\rm 3NF}|\Psi_{\rm rest}\rangle\Big).\end{aligned} \tag{3.15}$$

In this case there are significant contributions from both the zero- and one-body terms, while the two- and three-body terms are suppressed by a factor ε^2. Because of this it is possible to approximate the 3NF as

$$\hat{V}_{\rm 3NF} \approx W^{0b}_{\rm 3nf} + \hat{W}^{1b}_{\rm 3nf} \equiv \hat{V}^{\rm NO1B}_{\rm 3NF}. \tag{3.16}$$

This is what will be called the normal-ordering-one-body (NO1B)-approximation.

In case iii. the ground state can be written as

$$|\Psi_{\rm gs}\rangle = N\left(|\Psi_{\rm ref}\rangle + c_{1p-1h}\,|\Psi_{\rm 1p-1h}\rangle + c_{2p-2h}\,|\Psi_{\rm 2p-2h}\rangle + \varepsilon\,|\Psi_{\rm rest}\rangle\right), \tag{3.17}$$

where $N = \frac{1}{\sqrt{1+|c_{1p-1h}|^2+|c_{2p-2h}|^2+\varepsilon^2}}$,

$$|\Psi_{\rm 2p-2h}\rangle = \sum_{p_1,p_2\notin R}\sum_{h_1,h_2\in R}\xi_{p_1,p_2,h_1,h_2}\hat{c}^\dagger_{p_1}\hat{c}^\dagger_{p_2}\hat{c}_{h_2}\hat{c}_{h_1}\,|\Psi_{\rm ref}\rangle \tag{3.18}$$

is a normalized sum over $2p-2h$ excitations, c_{1p-1h} and c_{2p-2h} are of absolut magnitude of order one and $\varepsilon > 0$ is small. The ground-state expectation value becomes

$$\begin{aligned}\langle\Psi_{\rm gs}|\hat{V}_{\rm 3NF}|\Psi_{\rm gs}\rangle =& W^{0b}_{\rm 3NF} \\ &+ N^2|c_{1p-1h}|^2\,\langle\Psi_{\rm 1p-1h}|\hat{W}^{1b}_{\rm 3NF}|\Psi_{\rm 1p-1h}\rangle \\ &+ N^2|c_{2p-2h}|^2\,\langle\Psi_{\rm 2p-2h}|\hat{W}^{1b}_{\rm 3NF}+\hat{W}^{2b}_{\rm 3NF}|\Psi_{\rm 2p-2h}\rangle \\ &+ N^2\varepsilon^2\Big(\,\langle\Psi_{\rm rest}|\hat{W}^{1b}_{\rm 3NF}|\Psi_{\rm rest}\rangle \\ &+\,\langle\Psi_{\rm rest}|\hat{W}^{2b}_{\rm 3NF}|\Psi_{\rm rest}\rangle \\ &+\,\langle\Psi_{\rm rest}|\hat{W}^{3b}_{\rm 3NF}|\Psi_{\rm rest}\rangle\Big).\end{aligned} \tag{3.19}$$

The only term that is suppressed by ε^2 is the three-body term, all the zero-, one- and two-body term have all a significant contribution to the ground-state expectation

value of the 3NF. Therefore, the NO2B-approximation of the 3NF can be written as

$$\hat{V}_{\mathrm{3NF}} \approx W^{0b}_{\mathrm{3nf}} + \hat{W}^{1b}_{\mathrm{3nf}} + \hat{W}^{2b}_{\mathrm{3nf}} \equiv \hat{V}^{\mathrm{NO2B}}_{\mathrm{3NF}}. \tag{3.20}$$

In figure 3.1 the different many-body configurations are illustrated by showing the $|\Psi_{\mathrm{ref}}\rangle$, one-particle one-hole, two-particle two-hole and three-particle three-hole excitations of ^{4}He.

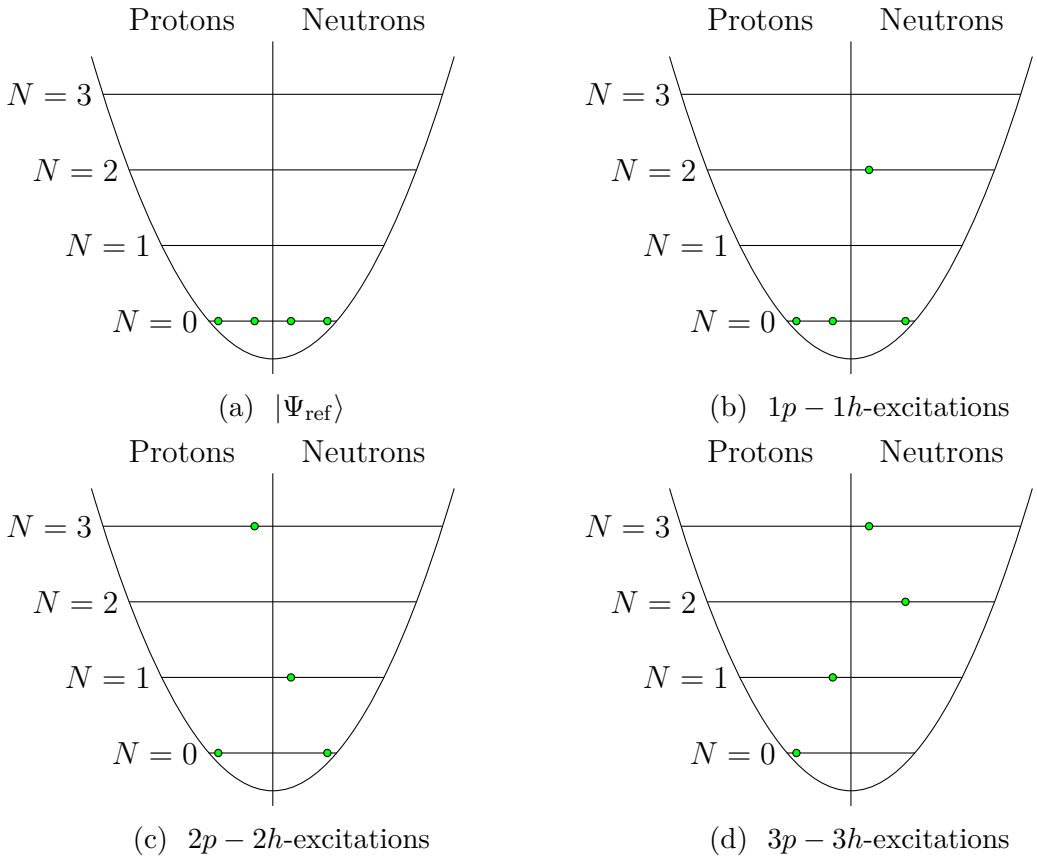

(a) $|\Psi_{\mathrm{ref}}\rangle$ (b) $1p-1h$-excitations

(c) $2p-2h$-excitations (d) $3p-3h$-excitations

Figure 3.1: Reference state (panel a), one-particle one-hole (panel b), two-particle two-hole (panel c) and three-particle three-hole (panel d) excitations of the reference state of ^{4}He. In the NO2B-approximation it is assumed that the contributions of three-particle three-hole excitations to the ground state expectation value of the 3NF potential are significantly smaller than the contributions of the other three.

3.1.3 Vacuum normal ordering

In order to use these approximate potentials, $\hat{V}_{\rm 3NF}^{{\rm NO}k{\rm B}}$ for $k = 0, 1, 2$, in the NCSM it is necessary to express them in a vacuum normal-ordered form. Vacuum normal-ordering implies that the reference state is the Fock state with no particles $|\rangle$. This means that all creation operators, $\hat{c}_\alpha^\dagger$, are moved to the left and all the annihilation operators, $\hat{c}_\alpha$, are moved to the right. The constant $W_{\rm 3NF}^{0b}$ is already in vacuum-normal ordered form, for this reason, I can focus on $\hat{W}_{\rm 3NF}^{1b}$ and $\hat{W}_{\rm 3NF}^{2b}$.

The one-body part, as defined in equation (3.9), is written as

$$\hat{W}_{\rm 3NF}^{1b} = \frac{1}{2}\sum_{\alpha,\alpha'}\sum_{\beta,\gamma\in R}\langle\alpha,\beta,\gamma|\hat{V}_{\rm 3NF}|\alpha',\beta,\gamma\rangle\left\{\hat{c}_\alpha^\dagger\hat{c}_{\alpha'}\right\}. \tag{3.21}$$

The normal-ordered factor $\left\{\hat{c}_\alpha^\dagger\hat{c}_{\alpha'}\right\}$ is related to $\hat{c}_\alpha^\dagger\hat{c}_{\alpha'}$ through the definition of contractions in equation 3.4. Thus, I have that $\left\{\hat{c}_\alpha^\dagger\hat{c}_{\alpha'}\right\} = \hat{c}_\alpha^\dagger\hat{c}_{\alpha'} - \delta_{\alpha,\alpha'\in R}$. The one-body part is therefore

$$\begin{aligned}\hat{W}_{\rm 3NF}^{1b} =& \frac{1}{2}\sum_{\alpha,\alpha'}\sum_{\beta,\gamma\in R}\langle\alpha,\beta,\gamma|\hat{V}_{\rm 3NF}|\alpha',\beta,\gamma\rangle\,\hat{c}_\alpha^\dagger\hat{c}_{\alpha'} \\ &- \frac{1}{2}\sum_{\alpha,\beta,\gamma\in R}\langle\alpha,\beta,\gamma|\hat{V}_{\rm 3NF}|\alpha,\beta,\gamma\rangle\,.\end{aligned} \tag{3.22}$$

The two-body part, found in equation (3.9) is written as

$$\hat{W}_{\rm 3NF}^{2b} = \frac{1}{4}\sum_{\substack{\alpha,\beta\\ \alpha',\beta'}}\sum_{\gamma\in R}\langle\alpha,\beta,\gamma|\hat{V}_{\rm 3NF}|\alpha',\beta',\gamma\rangle\left\{\hat{c}_\alpha^\dagger\hat{c}_\beta^\dagger\hat{c}_{\beta'}\hat{c}_{\alpha'}\right\}. \tag{3.23}$$

In this case the normal-ordered part, $\left\{\hat{c}_\alpha^\dagger\hat{c}_\beta^\dagger\hat{c}_{\beta'}\hat{c}_{\alpha'}\right\}$, is related to $\hat{c}_\alpha^\dagger\hat{c}_\beta^\dagger\hat{c}_{\beta'}\hat{c}_{\alpha'}$ through Wick's theorem,

$$\begin{aligned}\hat{c}_\alpha^\dagger\hat{c}_\beta^\dagger\hat{c}_{\beta'}\hat{c}_{\alpha'} =& \left\{\hat{c}_\alpha^\dagger\hat{c}_\beta^\dagger\hat{c}_{\beta'}\hat{c}_{\alpha'}\right\} \\ &+ \delta_{\alpha,\alpha'\in R}\left\{\hat{c}_\beta^\dagger\hat{c}_{\beta'}\right\} + \delta_{\beta,\beta'\in R}\left\{\hat{c}_\alpha^\dagger\hat{c}_{\alpha'}\right\} \\ &- \delta_{\alpha,\beta'\in R}\left\{\hat{c}_\beta^\dagger\hat{c}_{\alpha'}\right\} - \delta_{\beta,\alpha'\in R}\left\{\hat{c}_\alpha^\dagger\hat{c}_{\beta'}\right\} \\ &+ \delta_{\alpha,\alpha'\in R}\delta_{\beta,\beta'\in R} - \delta_{\alpha,\beta'\in R}\delta_{\beta,\alpha'\in R}.\end{aligned} \tag{3.24}$$

Using the definition of contraction I now get that

$$\begin{aligned}\left\{\hat{c}^\dagger_\alpha \hat{c}^\dagger_\beta \hat{c}_{\beta'} \hat{c}_{\alpha'}\right\} =& \hat{c}^\dagger_\alpha \hat{c}^\dagger_\beta \hat{c}_{\beta'} \hat{c}_{\alpha'} \\ &- \delta_{\alpha,\alpha'\in R} \hat{c}^\dagger_\beta \hat{c}_{\beta'} - \delta_{\beta,\beta'\in R} \hat{c}^\dagger_\alpha \hat{c}_{\alpha'} \\ &+ \delta_{\alpha,\beta'\in R} \hat{c}^\dagger_\beta \hat{c}_{\alpha'} + \delta_{\beta,\alpha'\in R} \hat{c}^\dagger_\alpha \hat{c}_{\beta'} \\ &+ \delta_{\alpha,\alpha'\in R}\delta_{\beta,\beta'\in R} - \delta_{\alpha,\beta'\in R}\delta_{\beta,\alpha'\in R}.\end{aligned} \tag{3.25}$$

The two-body part in vacuum-normal-ordered form is therefore

$$\begin{aligned}\hat{W}^{2b}_{\mathrm{3NF}} =& \frac{1}{4} \sum_{\substack{\alpha,\beta \\ \alpha',\beta'}} \sum_{\gamma\in R} \langle \alpha,\beta,\gamma|\hat{V}_{\mathrm{3NF}}|\alpha',\beta',\gamma\rangle \, \hat{c}^\dagger_\alpha \hat{c}^\dagger_\beta \hat{c}_{\beta'} \hat{c}_{\alpha'} \\ &- \sum_{\alpha,\alpha'} \sum_{\beta,\gamma\in R} \langle \alpha,\beta,\gamma|\hat{V}_{\mathrm{3NF}}|\alpha',\beta,\gamma\rangle \, \hat{c}^\dagger_\alpha \hat{c}_{\alpha'} \\ &+ \frac{1}{2} \sum_{\alpha,\beta,\gamma\in R} \langle \alpha,\beta,\gamma|\hat{V}_{\mathrm{3NF}}|\alpha,\beta,\gamma\rangle \, .\end{aligned} \tag{3.26}$$

I can now combine these results and set up the three approximate potentials in vacuum-normal-ordered form, and get

$$\hat{V}^{\mathrm{NO0B}}_{\mathrm{3NF}} = \frac{1}{6} \sum_{\alpha,\beta,\gamma\in R} \langle \alpha,\beta,\gamma|V_{\mathrm{3NF}}|\alpha,\beta,\gamma\rangle \, , \tag{3.27}$$

$$\begin{aligned}\hat{V}^{\mathrm{NO1B}}_{\mathrm{3NF}} =& \frac{1}{2} \sum_{\alpha,\alpha'} \sum_{\beta,\gamma\in R} \langle \alpha,\beta,\gamma|\hat{V}_{\mathrm{3NF}}|\alpha',\beta,\gamma\rangle \, \hat{c}^\dagger_\alpha \hat{c}_{\alpha'} \\ &- \frac{1}{3} \sum_{\alpha,\beta,\gamma\in R} \langle \alpha,\beta,\gamma|\hat{V}_{\mathrm{3NF}}|\alpha,\beta,\gamma\rangle \, ,\end{aligned} \tag{3.28}$$

$$\begin{aligned}\hat{V}^{\mathrm{NO2B}}_{\mathrm{3NF}} =& \frac{1}{4} \sum_{\substack{\alpha,\beta \\ \alpha',\beta'}} \sum_{\gamma\in R} \langle \alpha,\beta,\gamma|\hat{V}_{\mathrm{3NF}}|\alpha',\beta',\gamma\rangle \, \hat{c}^\dagger_\alpha \hat{c}^\dagger_\beta \hat{c}_{\beta'} \hat{c}_{\alpha'} \\ &- \frac{1}{2} \sum_{\alpha,\alpha'} \sum_{\beta,\gamma\in R} \langle \alpha,\beta,\gamma|\hat{V}_{\mathrm{3NF}}|\alpha',\beta,\gamma\rangle \, \hat{c}^\dagger_\alpha \hat{c}_{\alpha'} \\ &+ \frac{1}{6} \sum_{\alpha,\beta,\gamma\in R} \langle \alpha,\beta,\gamma|\hat{V}_{\mathrm{3NF}}|\alpha,\beta,\gamma\rangle \, .\end{aligned} \tag{3.29}$$

In conclusion, the NO2B-Hamiltonian is

$$\hat{H}^{\mathrm{NO2B}} = \hat{T}_{\mathrm{int}} + \hat{V}_{\mathrm{2NF}} + \hat{V}^{\mathrm{NO2B}}_{\mathrm{3NF}}. \tag{3.30}$$

3.2 Closed-core reference state

Every approximation comes with some cost. The SR-NO2B-approximation has several costs, of which the breaking of translational symmetry and the limitation to closed-core nuclei are the most severe ones. In this section I will focus on the latter, the limitation to closed-core nuclei, while chapter 4 focuses on the former.

There is nothing in the definition of the single-reference NO2B-approximation that prohibits its use for any nucleus with $A \geq 3$. However, if the nucleus is not closed-core, there exists multiple Slater-determinants that all have the lowest possible HO-energy. Take the ^{3}He nucleus as an example. It has three nucleons, two protons and one neutron, that all can be placed in the lowest HO-shell. However, there are two possible neutron states, $\left|n = 0, l = 0, j = \frac{1}{2}, m = \pm\frac{1}{2}\right\rangle$, which gives us two possible Slater-determinants, with the same HO-energy, that can be chosen as a reference state. For larger nuclei the number of possible reference states can be much greater, for instance, for ^{6}Li there are 36 equally valid configurations and none of them can be preferred over the others as a reference state.

Closed-core nuclei on the other hand do only have one Slater-determinant with the lowest possible HO-excitation. Therefore, there is no ambiguity in the choice of reference state. In this work I will only apply the NO2B-approximation to the two lowest closed-core nuclei: ^{4}He and ^{16}O.

3.3 Benchmarking the approximated three-nucleon force

Up to this point I have derived three different approximation schemes of 3NFs: NO0B, NO1B and NO2B. However, so far little or no legitimacy of these approximations has been presented. In this section I intend to determine if all, any or none of these approximation-schemes can be useful in real calculations. For this reason I have chosen to benchmark the three schemes by computing the ground-state energy of the ^{4}He nucleus using a state-of-the-art nuclear interaction from χEFT.

The ^{4}He is the lightest closed-core nucleus and is therefore a good candidate for a benchmark. The choice of reference state is not ambiguous, I simply fill the lowest HO-shell ($n = l = 0$ for all four nucleons). Furthermore, the ^{4}He nucleus is also small enough for full inclusion of 3NFs up to very large NCSM-model spaces. It is therefore possible to compare the approximate calculations with exact ones.

To benchmark the NO0B, NO1B and NO2B-approximations, I computed the ground-state energy of ^{4}He for each of them and compared the results to the ground-

state energy computed with the full 3NF using NCSM with a basis frequency $\hbar\omega = 20\,\text{MeV}$. In all cases 2NFs and 3NFs derived from the NNLO-sat interaction [17] has been used. The result of these calculations can be viewed in figure 3.2. The green dotted curve corresponds to the NO0B-approximated 3NFs, the orange dashed curve corresponds to the NO1B-approximated 3NFs and the blue dash-dotted curve corresponds to the NO2B-approximated 3NFs, the black solid curve is computed with full inclusion of 3NFs. The pAntoine code [24] has been used for the NCSM-calculations for each of the three approximations, while the ns-opt code [27], an implementation of Jacobi-NCSM [28], has been utilized for the NCSM-calculations with full inclusion of 3NFs and the fully converged ground-state energy.

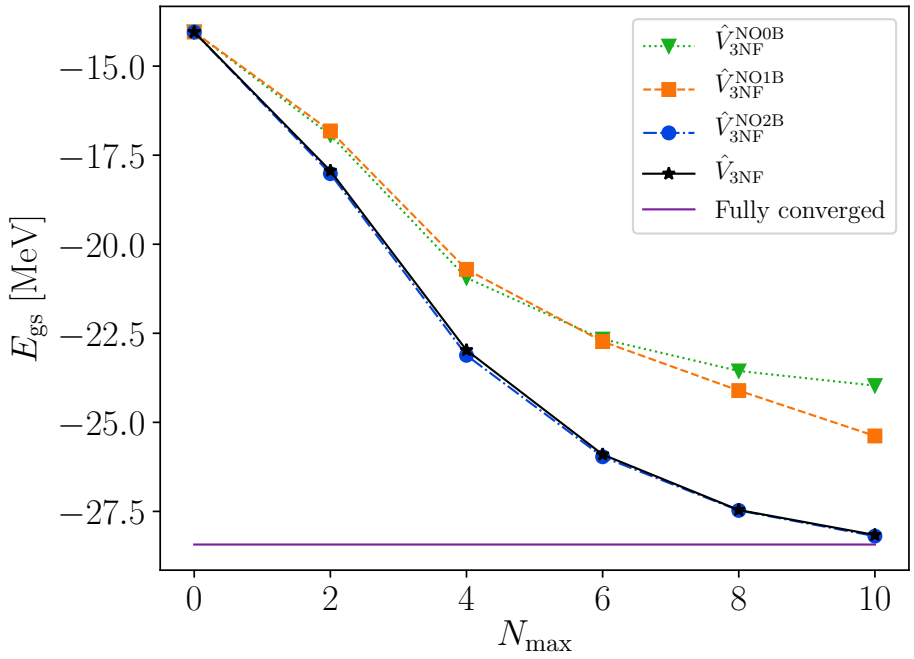

Figure 3.2: Benchmark plot of the NO0B-, NO1B and NO2B-approximations. The ground-state energy of ^{4}He for each level of approximation and with full inclusion of 3NFs. The 2NFs and 3NFs used for these calculations are derived from the NNLO-sat interaction [17].

As can be seen in figure 3.2 neither the NO0B nor the NO1B curves are close to the full 3NF result, indicating that $k\text{p} - k\text{h}$-excitations out of the reference state for $k > 1$ are a significant part of the full ground-state. However, the NO2B curve is very

close to the full 3NF result indicating that inclusion of up to 2p − 2h-excitations gives a sufficient description of the ^{4}He ground-state energy, at least for this particular choice of many-body basis.

I therefore conclude that the NO0B and NO1B approximations are not sufficient to describe the physics of 3NFs in light atomic nuclei. For this reason I will henceforth only consider the NO2B approximation.

3.4 The computer implementation - cNO2B

A product of this work is an implementation of the NOkB-approximations presented in section 3.1 as a C program. This is a rewrite of a prototype Python code that was developed as part of a master thesis written by Fahlin Strömberg [29].

The program, called cNO2B, reads 3NFs in M-scheme and computes an effective 2NF using either the NO0B-, NO1B- or NO2B-approximation. The resulting matrix elements are JT-coupled [30], and added to a preexisting file with JT-coupled 2NF matrix elements. The generated 2NF elements are stored to file and can be directly used by pAntoine [24].

Note that the NO0B, NO1B, and NO2B potentials do not correspond to pure two-body operators. Therefore, the one- and zero-body terms, in equations (3.27), (3.28) and (3.29), are transformed to equivalent two-body operators for the given A-body system by insertion of sufficiently many identity operators. For example, the one body terms has the form

$$\sum_{\alpha,\alpha'} \sum_{\beta,\gamma\in R} \langle \alpha,\beta,\gamma|\hat{V}_{\mathrm{3NF}}|\alpha',\beta,\gamma\rangle\, \hat{c}^\dagger_\alpha \hat{c}_{\alpha'}. \tag{3.31}$$

Assuming that the nucleus has A nucleons, then by inserting

$$I_{A-1} = \frac{1}{A-1}\sum_{\delta} \hat{c}^\dagger_\delta \hat{c}_\delta, \tag{3.32}$$

which is an identity operator for the $A-1$ nucleon system, between the two creation and annihilation operators the one-body term is

$$\sum_{\alpha,\alpha',\delta} \sum_{\beta,\gamma\in R} \frac{\langle \alpha,\beta,\gamma|\hat{V}_{\mathrm{3NF}}|\alpha',\beta,\gamma\rangle}{A-1} \hat{c}^\dagger_\alpha \hat{c}^\dagger_\delta \hat{c}_\delta \hat{c}_{\alpha'}, \tag{3.33}$$

which is a two-nucleon force.

The main reason I want to approximate 3NFs is to reduce the computational cost of performing calculations with realistic interactions in the NCSM. In section 2.2

I established the enormous difference in computational cost between only including 2NFs and including both 2NFs and 3NFs in the NCSM. From hours in the 2NF case to predicted months in the 3NF case. The NO2B procedure might be computationally heavy, however, and thus reduce the time benefit of doing NCSM with only 2NFs. I have therefore plotted the wall time of cNO2B as a function of $N_{\max}$ in figure 3.3 for both ^{4}He and ^{16}O. These speed measurements have been performed on the same type of computer as used in 2.2.

While the wall time of cNO2B increases roughly exponentially for both nuclei the maximum execution times are still relatively low. The maximum wall time for ^{16}O at $N_{\max} = 8$ is about three minutes. This can be compared to the eight hours that pAntoine needed to solve the MBSE with 2NFs in this model space, and the predicted two months if including a 3NF[1]. Thus, I conclude that the NO2B-approximation does not add significant computational complexity.

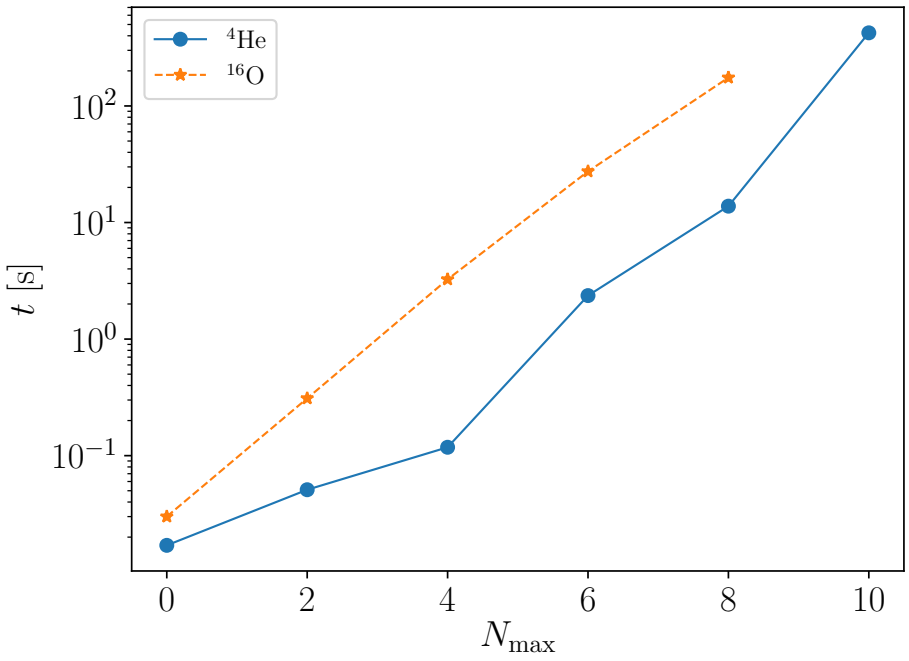

Figure 3.3: Wall time for performing the NO2B-approximation with the cNO2B code for ^{4}He core and ^{16}O core reference state.

[1]As mentioned earlier, pAntoine can not include 3NFs. This prediction is about a hypotetical NCSM code that works similarly to pAntoine but can include 3NFs.

In figure 3.4 I have plotted the maximum RAM memory usage for cNO2B for both ^{4}He and ^{16}O as a function of $N_{\max}$. For all $N_{\max} = 0, 2, 4, 6, 8, (10)$, where $N_{\max} = 10$ is only included for ^{4}He, the peak memory usage is lower than 60 GB, which is well within the RAM size of a single node on the computer I used.

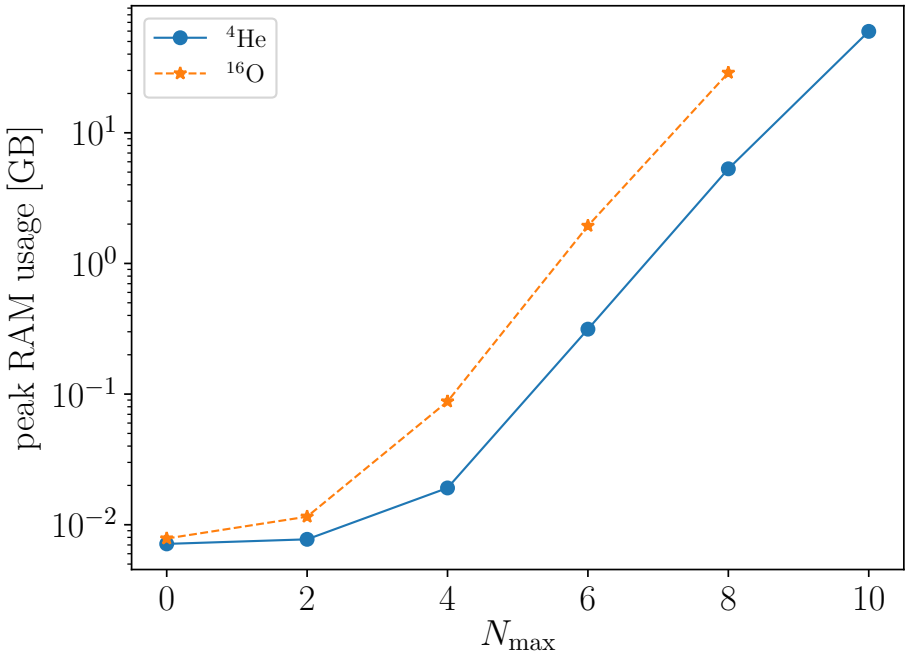

Figure 3.4: Peak RAM usage of cNO2B for a ^{4}He core and ^{16}O core reference state.

The cNO2B code requires the 3NF matrix elements to be expressed in the M-scheme format, meaning that the angular momentum of each particle is not coupled to a collective angular momentum. While it is certainly possible to express the NO2B approximation in J-scheme [31], I choose not to do so as a first proof of concept implementation. However, implementing NO2B in M-scheme comes with a penalty in memory usage. The number of matrix elements can be significantly reduced in J-scheme since the 3NF-operator is a scalar one and can be rewritten using the Wigner-Eckart theorem.

Figure 3.5 illustrates how fast the M-scheme 3NF matrix grows in size. The disk space needed to store the matrix elements as a HDF5 file is plotted for different truncations. Here $N_{\max}$ refers to the model size of the three-body NCSM basis used to span the 3NFs. Note that the vertical axis is in logarithmic scale and that the

curve is close to be linear, hence the storage size increases almost exponentially with $N_{\max}$. Since the size increases more than a decade between $N_{\max} = 8$ and $N_{\max} = 10$ (from 7.9 GB to 96 GB), and that it is likely to continue to do so, a $N_{\max} = 12$ file would require approximately 1.14 TB. For this reason I limit this work to $N_{\max} = 10$ for ^{4}He and $N_{\max} = 8$ for ^{16}O.

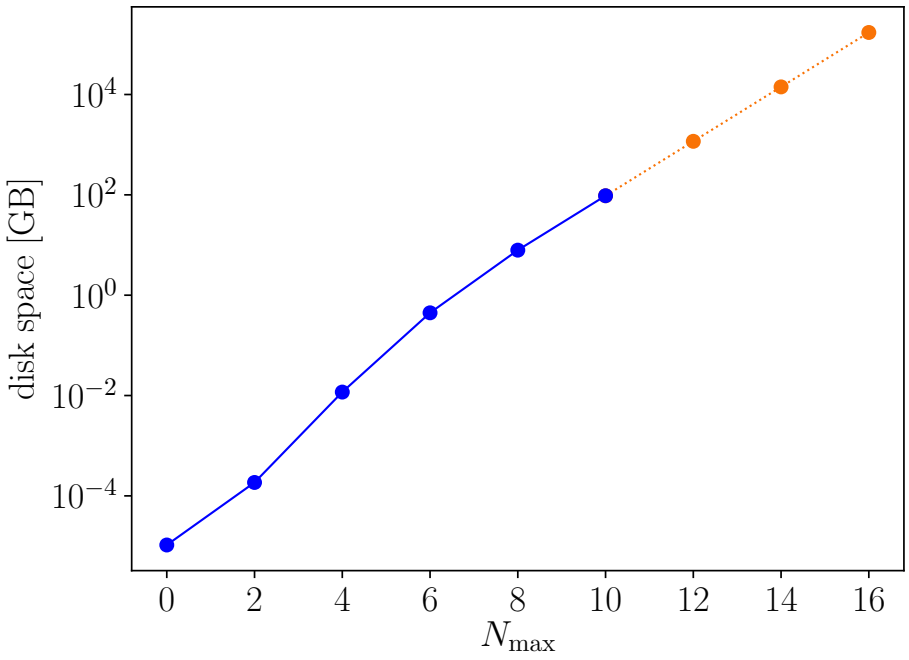

Figure 3.5: File size for explicitly storing the 3NFs in M-scheme on disk in HDF5 format. The blue solid curve corresponds to actual data files produced and used in this work while the orange doted curve is an exponential extrapolation to larger model spaces. Observe the logarithmic scale on the disk space axis.

Chapter 4

The Center of Mass Problem

Nuclear structure does not depend on where the nucleus is located in space since the nucleus is a self-bound system. This is characterized by the Hamiltonian considered in this work, equation (2.2), through its translational symmetry. When the exact Hamiltonian is used in the NCSM-method this translational symmetry yields eigenstates that are product states of intrinsic excitations and CM-excitations. Thus, the method is able to separate internal from external dynamics.

However, when using the NO2B Hamiltonian, equation (3.30), the approximated 3NF is no longer translation invariant and it is not guaranteed that the NCSM-eigenstates separate CM- from intrinsic-excitations. The goal of this chapter is to discuss the origin of the CM-problem in the NO2B-approximation, and to explore two ways to measure its consequences.

In section 4.1, the separation of CM and intrinsic excitations in the NCSM given a translationally symmetric Hamiltonian is discussed. The translational symmetry breaking of the NO2B-approximation is demonstrated in section 4.2. Finally, Section 4.3 introduces two metrics to measure CM-contamination in the ground state.

4.1 The Center of Mass separation in the No Core Shell Model

The Hamiltonian considered in this work, equation (2.2), has both translational and rotational symmetry. When solving the MBSE approximately, using some truncated many-body basis, there is no guarantee in general that these symmetries will be conserved. Rotational symmetry can be maintained by using an eigenbasis to the total angular-momentum operator. However, to correctly deal with translational

symmetry for a general basis, relative (Jacobi)-coordinates are needed [8]. Unfortunately, since nucleons are fermions this basis must be constructed with antisymmetry under particle permutations, which makes it unpractical for large systems [8].

As described in chapter 2 the NCSM utilizes a finite HO eigenbasis, which is truncated on the total number of HO-excitations above the lowest possible configuration. It can be shown that the NCSM-basis respects the translational symmetry of the Hamiltonian by yielding eigenstates that separates into an intrinsic and CM part[1] [32]. This is expressed as

$$\begin{aligned}\langle \vec{r}_1, \cdots, \vec{r}_A, \sigma_1, \cdots, \sigma_A, \tau_1, \cdots, \tau_A | \Psi_{\mathrm{NCSM}} \rangle = \\ \langle \vec{\eta}_1, \cdots, \vec{\eta}_{A-1}, \sigma_1, \cdots, \sigma_A, \tau_1, \cdots, \tau_A | \Psi_{\mathrm{NCSM}} \rangle \phi_{\mathcal{N},\mathcal{L},\mathcal{M}}(\vec{R}_{\mathrm{CM}}),\end{aligned} \tag{4.1}$$

where $\vec{r}_k$, σ_k and τ_k are the lab-coordinate position, spin and isospin of particle k, $\vec{\eta}_k$ is the kth intrinsic Jacobi coordinate, $\vec{R}_{\mathrm{CM}}$ is the CM coordinate and $\phi_{\mathcal{N},\mathcal{L},\mathcal{M}}(\vec{r})$ is a HO-state wave function [8]. Through this separation, it is possible to study the intrinsic state although working in a lab-coordinate basis.

4.2 The Center of Mass problem in the NO2B-approximation

The NO2B-approximation of 3NFs was introduced in chapter 3. However, there is a serious problem needed to be discussed. The NO2B-approximation breaks the translational symmetry of the Hamiltonian.

While the 3NF potential only depends on intrinsic coordinates, the reference state has a Gaussian dependence on the CM-coordinate, see equation (4.1). This CM-dependence will propagate into the approximate potentials, $\hat{V}_{\mathrm{3NF}}^{\mathrm{NO}k\mathrm{B}}$ for $k = 1, 2$, which will therefore break the translational symmetry.

Let us consider a specific example, namely the ^{4}He nucleus. The reference state has all four nucleons in the lowest harmonic oscillator state since there are four degenerate spin and isospin states in this case. Therefore, the spatial part of the reference wave function is

$$\langle \vec{r}_1, \vec{r}_2, \vec{r}_3, \vec{r}_4 | \Psi_{\mathrm{ref}} \rangle_{\mathrm{spat}} = N e^{-\frac{m\omega}{2\hbar}\left(\vec{r}_1^{\,2} + \vec{r}_2^{\,2} + \vec{r}_3^{\,2} + \vec{r}_4^{\,2}\right)}, \tag{4.2}$$

where $\vec{r}_1$ through $\vec{r}_4$ are the lab coordinates of the four nucleons and N is a normalization constant. The antisymmetry of the Slater determinant is manifest in the

[1] This property is related to the total-energy truncated sums that appear in the Brody-Moshinsky transfromation between laboratory and relative coordinates

spin isospin part of the state, excluded above. We can introduce a set of Jacobi-coordinates,

$$\vec{R}_{\mathrm{CM}} = \frac{1}{4}\left(\vec{r}_1 + \vec{r}_2 + \vec{r}_3 + \vec{r}_4\right) \tag{4.3}$$

$$\vec{\eta}_1 = \vec{r}_2 - \vec{r}_1 \tag{4.4}$$

$$\vec{\eta}_2 = \vec{r}_3 - \frac{1}{2}\left(\vec{r}_1 + \vec{r}_2\right) \tag{4.5}$$

$$\vec{\eta}_3 = \vec{r}_4 - \frac{1}{3}\left(\vec{r}_1 + \vec{r}_2 + \vec{r}_3\right), \tag{4.6}$$

where $\vec{\eta}_k$ for $k = 1, 2, 3$ are relative coordinates and $\vec{R}_{\mathrm{CM}}$ is the CM-coordinate. Transforming the spatial part of the reference wave function (4.2) to Jacobi coordinates yields

$$\left\langle \vec{\eta}_1, \vec{\eta}_2, \vec{\eta}_3, \vec{R}_{\mathrm{CM}} \middle| \Psi_{\mathrm{ref}} \right\rangle_{\mathrm{spat}} = N e^{-\frac{m\omega}{2\hbar}\left(4\vec{R}^2_{\mathrm{CM}} + \frac{1}{2}\vec{\eta}_1^2 + \frac{2}{3}\vec{\eta}_2^2 + \frac{3}{4}\vec{\eta}_3^2\right)}, \tag{4.7}$$

where the fractions arise from the corresponding reduced masses. Therefore, the reference state clearly depends on the CM-coordinate of the whole system.

Assuming that I were to translate the system along $\vec{d}$, as illustrated in figure 4.1, the reference state would move relative the CM of the nucleus along $-\vec{d}$. This would be equivalent with normal ordering the 3NF relative a new reference state with spatial wave function

$$\left\langle \vec{\eta}_1, \vec{\eta}_2, \vec{\eta}_3, \vec{R}_{\mathrm{CM}} \middle| \Psi'_{\mathrm{ref}} \right\rangle_{\mathrm{spat}} = N e^{-\frac{m\omega}{2\hbar}\left(4\vec{R}^2_{\mathrm{CM}} + \frac{1}{2}\vec{\eta}_1^2 + \frac{2}{3}\vec{\eta}_2^2 + \frac{3}{4}\vec{\eta}_3^2\right)} e^{-\frac{m\omega}{2\hbar}\left(4\vec{d}^2 - 8\vec{R}_{\mathrm{CM}}\cdot\vec{d}\right)}. \tag{4.8}$$

This new reference state $|\Psi'_{\mathrm{ref}}\rangle$ can not be expressed as a single Slater determinant in a HO-basis centred around origo but would rather require multi-reference normal-ordering.

Each of the one-, two- and three-body terms in the normal-ordered expansion of the 3NF, in equation (3.9), breaks the translational symmetry. However, since the full force is translationally invariant the symmetry breaking of each term cancel. However, when the three-body term, $\hat{W}^{3b}_{\mathrm{3NF}}$, is discarded, there is no longer a cancellation, and the approximated force breaks the symmetry.

It is clear from the example that translating the normal ordered 3NF is equivalent of normal ordering relative a different state, which in general is not a single HO Slater determinant. This proves that the NO2B-approximation is not translation invariant. As a consequence it is no longer guaranteed that the NCSM ground-state separates into a CM and an intrinsic state.

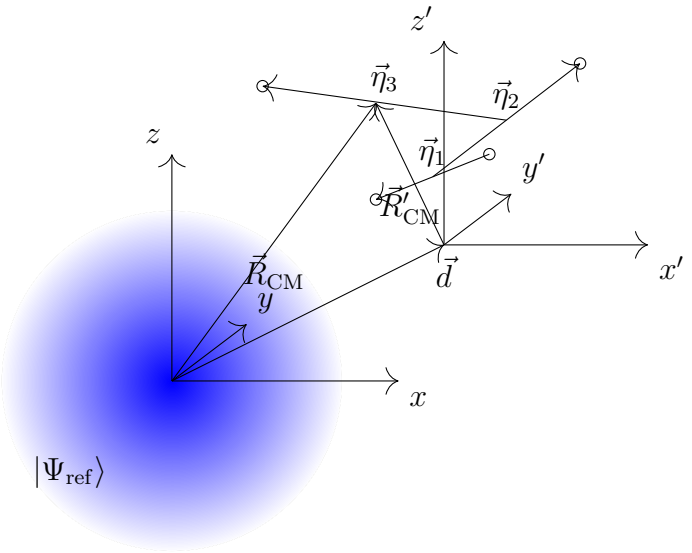

Figure 4.1: Translation of a normal ordered ^{4}He nucleus. The blue shadowed area represents the ^{4}He reference state in equation (4.2), the vector $\vec{d}$ represents the distance that the system has been translated.

4.3 Measuring Center of Mass mixing

As demonstrated, the NO2B-approximation breaks the translational symmetry of the Hamiltonian, and it is no longer guaranteed that the NCSM-method yields CM-separable eigenstates. Thus, we must expect a mixing between the CM- and the intrinsic-part of the eigenstates. In this section I will introduced two metrics that can be used to study such mixing.

When the NCSM eigenstate is separable, as in equation 4.1 it is a product state of an intrinsic and a CM-state expressed as

$$|\Psi_{\mathrm{NCSM}}\rangle = |\Psi_{\mathrm{int}}\rangle \otimes |\Psi_{\mathrm{CM}}\rangle \,. \tag{4.9}$$

In this case the CM can be said to be in a single quantum state $|\Psi_{\mathrm{CM}}\rangle$, which will be referred to as a pure quantum state [33]. The intrinsic-state is also a pure state $|\Psi_{\mathrm{int}}\rangle$.

If the NCSM eigenstate is not separable, it is an entangled state and can be written as a superposition of product states

$$|\Psi_{\mathrm{NCSM}}\rangle = \sum_{i,j} c_{i,j} \left|\Psi^i_{\mathrm{int}}\right\rangle \otimes \left|\Psi^j_{\mathrm{CM}}\right\rangle \tag{4.10}$$

where $|\Psi^i_{\text{int}}\rangle$ and $\left|\Psi^j_{\text{CM}}\right\rangle$ form two orthonormal bases, for intrinsic- and CM-excitations respectively. It is not possible to construct pure quantum states for either the CM- nor the intrinsic-state in this case. Instead, there exists a range of quantum states, $\left|\Psi^j_{\text{CM}}\right\rangle$, that the CM can be in with a probability p_j, and similar for the intrinsic system. This will be referred to as a mixed quantum state and is best described with density matrices [33]. Assuming that the state in equation (4.10) is normalized, the corresponding density matrix for the whole system is

$$\hat{\rho}_{\text{NCSM}} = |\Psi_{\text{NCSM}}\rangle \langle\Psi_{\text{NCSM}}| . \tag{4.11}$$

By a partial trace of $\hat{\rho}_{\text{NCSM}}$ over the intrinsic Hilbert space the CM density matrix can be determined to be

$$\hat{\rho}_{\text{CM}} = \sum_{i,j,k} c_{i,j} c^*_{i,k} \left|\Psi^j_{\text{CM}}\right\rangle \left\langle\Psi^k_{\text{CM}}\right| . \tag{4.12}$$

Similarly the intrinsic density matrix can be shown to be

$$\hat{\rho}_{\text{int}} = \sum_{i,j,k} c_{j,i} c^*_{k,i} \left|\Psi^j_{\text{int}}\right\rangle \left\langle\Psi^k_{\text{int}}\right| . \tag{4.13}$$

Density matrices can also be used in the separable case. If the NCSM-eigenstate is separable, that is the CM state is a pure quantum state, it can be shown that $\text{tr}\{\hat{\rho}^2_{\text{CM}}\} = 1$. In fact $\text{tr}\{\hat{\rho}^2_{\text{CM}}\} = 1$ if and only if the CM-state is a pure quantum state, see appendix section B.2 for proof. Therefore, the quantity $\text{tr}\{\hat{\rho}^2_{\text{CM}}\}$ could be used as a measure of how much CM mixing there is in the eigenstate. Unfortunately, computing the CM density matrix is extremely demanding and is not practical for larger systems. This suggests a need for alternatives. In this section I will present two different methods to measure to the CM-mixing: *The N_{CM} measure* (section 4.3.1) and *the ξ_{CM} measure* (section 4.3.2).

4.3.1 The N_{CM} measure

This method has been previously discussed in the context of the Coupled-Cluster (CC) method by Hagen, Papenbrock and Dean [34]. In their case the translational symmetry is not necessarily broken by the Hamiltonian, but rather broken by the choice of the Hartree-Fock basis. Despite this difference in origin of the symmetry breaking, their method can be used to analyse the CM-mixing from the NO2B-approximation.

Let us assume that the ground state is separable according to equation (4.9),

$$|\Psi_{\text{gs}}\rangle = |\Psi_{\text{gs}-\text{int}}\rangle \otimes |\Psi_{\text{gs}-\text{CM}}\rangle \tag{4.14}$$

where $|\Psi_{\text{gs}-\text{CM}}\rangle$ is the ground state of a shifted HO-Hamiltonian

$$\hat{H}_{\text{CM}}(\tilde{\omega}) = \hat{H}_{\text{HO}-\text{CM}} - \frac{3\hbar\tilde{\omega}}{2} = \hat{T}_{\text{CM}} + \frac{Am\tilde{\omega}^2}{2}\hat{R}^2_{\text{CM}} - \frac{3\hbar\tilde{\omega}}{2} \tag{4.15}$$

for some frequency $\tilde{\omega}$ that is not necessarily equal to the basis-frequency ω. It can be noted that

$$\hat{H}_{\text{CM}}(\omega) + \frac{3}{2}\hbar\omega - \hat{T}_{\text{CM}} = \frac{\omega^2}{\tilde{\omega}^2}\left(\hat{H}_{\text{CM}}(\tilde{\omega}) + \frac{3}{2}\hbar\tilde{\omega} - \hat{T}_{\text{CM}}\right). \tag{4.16}$$

Taking the expectation value with respect to $|\Psi_{\text{gs}}\rangle$ gives that

$$\langle\hat{H}_{\text{CM}}(\omega)\rangle + \frac{3}{2}\hbar\omega - \frac{3\hbar\tilde{\omega}}{4} = \frac{\omega^2}{\tilde{\omega}^2}\left(\langle\hat{H}_{\text{CM}}(\tilde{\omega})\rangle + \frac{3}{2}\hbar\tilde{\omega} - \frac{3\hbar\tilde{\omega}}{4}\right), \tag{4.17}$$

where I have exploited that $\langle T_{\text{CM}}\rangle = \frac{3\hbar\tilde{\omega}}{4}$ by my assumption. The expectation value $\langle\hat{H}_{\text{CM}}(\tilde{\omega})\rangle$ is zero since $|\Psi_{\text{gs}-\text{CM}}\rangle$ is the ground state of $\hat{H}_{\text{CM}}(\tilde{\omega})$ by assumption. Solving for $\hbar\tilde{\omega}$ yields

$$\hbar\tilde{\omega}^{\pm} = \hbar\omega + \frac{2}{3}\langle\hat{H}_{\text{CM}}(\omega)\rangle \pm \sqrt{\frac{4}{9}\langle\hat{H}_{\text{CM}}(\omega)\rangle^2 + \frac{4}{3}\hbar\omega\langle\hat{H}_{\text{CM}}(\omega)\rangle}. \tag{4.18}$$

To test the assumption in equation (4.14) I compute $\langle\hat{H}_{\text{CM}}(\tilde{\omega}^{\pm})\rangle$ for each of the two solutions in equation (4.18) yielding $E^{\pm}_{\text{CM}}$. If $E^{+}_{\text{CM}} > E^{-}_{\text{CM}}$ I let $\tilde{\omega} = \tilde{\omega}^{+}$ otherwise $\tilde{\omega} = \tilde{\omega}^{-}$. I will henceforth refer to $\tilde{\omega}$ obtained by this method as $\tilde{\omega}_N$.

The quantity $N_{\text{CM}} = \frac{\langle\hat{H}_{\text{CM}}(\tilde{\omega}_N)\rangle}{\hbar\tilde{\omega}_N}$ can now be considered a measure of how well the assumption in (4.14) holds. If $N_{\text{CM}} = 0$, the assumption holds exactly. For large N_{CM} I will consider the assumption broken.

4.3.2 The ξ_{CM} measure

The second method has previously been used in the context of the in-medium similarity-renomalization group (IM-SRG) method [35]. In IM-SRG the breaking of the translational symmetry arises due to the choice of a different truncation of the HO-basis than in the NCSM. Instead of limiting the total HO-excitation, the single-particle HO-excitation is limited. Therefore, there is no guarantee that the eigenstates of a translation-invariant Hamiltonian separates the CM- and intrinsic-excitations.

The central idea behind the ξ_{CM} method is to compute the quantity

$$\xi_{\text{CM}} = \frac{\sqrt{\langle \hat{P}^2_{\text{CM}} \rangle \langle \hat{R}^2_{\text{CM}} \rangle}}{\hbar} - \frac{3}{2}, \tag{4.19}$$

where $\hat{P}_{\text{CM}}$ is CM-momentum and $\hat{R}_{\text{CM}}$ is the CM-position.

If the CM-part of the ground state is a HO-state with HO-length $b = \sqrt{\frac{\hbar}{Am\tilde{\omega}}}$, radial quantum number $\mathcal{N}$ and angular momentum quantum number $\mathcal{L}$ then the expectation values are

$$\langle \hat{P}^2_{\text{CM}} \rangle = \frac{\hbar^2}{b^2} \left(2\mathcal{N} + \mathcal{L} + \frac{3}{2} \right), \tag{4.20}$$

$$\langle \hat{R}^2_{\text{CM}} \rangle = b^2 \left(2\mathcal{N} + \mathcal{L} + \frac{3}{2} \right), \tag{4.21}$$

and therefore

$$\xi_{\text{CM}} = 2\mathcal{N} + \mathcal{L}. \tag{4.22}$$

It is, therefore, clear that if the CM-part of the ground state is a HO-ground-state then $\xi_{\text{CM}} = 0$. Furthermore, the HO-frequency of the CM-part in a HO-ground-state can be computed by

$$\hbar\tilde{\omega}_\xi = \frac{4}{3} \langle T_{\text{CM}} \rangle. \tag{4.23}$$

The metric ξ_{CM} is always positive, as proven in appendix B.1. I will, therefore, consider the situation $\xi_{\text{CM}} \ll 1$ to be a sign that $|\Psi_{\text{gs}}\rangle$ separates into an intrinsic state and a CM-HO ground-state.

4.3.3 Limitations of the measures

None of the measures, introduced previously, can measure the CM-mixing in every situation. In this subsection I intend to explore in which circumstances, if any, it is possible to determine a separation with these two metrics and when it is indeterminable.

In the investigation in appendix A, I establish that the only case when it is possible to say something about whether the NCSM-ground state $|\Psi_{\text{gs}}\rangle$ separates or mixes CM- and intrinsic excitations, is if $N_{\text{CM}} = 0$ and $\xi_{\text{CM}} = 0$. If these measures are zero the CM-state is a pure HO-ground state, in all other cases it really is not possible to make conclusive claims. Therefore, I will only consider close to zero values as signs of CM-separation.

A different limitation has to do with representing a HO-ground state with a frequency $\tilde{\omega}$ in a finite HO-basis with a different frequency ω. In an infinite HO-basis the ground state of any HO-operator with any frequency $\tilde{\omega} > 0$ is exactly representable. However, a HO state with frequency $\tilde{\omega}$ can not be exactly represented in a truncated HO-basis with a frequency ω such that $\tilde{\omega} \neq \omega$.

To illustrate this limitation, I have computed the ground state of

$$H_{\text{HO}-\text{CM}} = \frac{P_{\text{CM}}^2}{2Am} + \frac{Am\tilde{\omega}}{2} R_{\text{CM}}^2 \tag{4.24}$$

in a ^{4}He NCSM basis with a frequency ω for different values of $N_{\max}$.

The N_{CM} meauser computed for the ground state of $H_{\text{HO}-\text{CM}}$ as a function of $\frac{\tilde{\omega}}{\omega}$ is plotted in figure 4.2. In figure 4.3 the measure ξ_{CM} computed for the same state is plotted, also as a function of $\frac{\tilde{\omega}}{\omega}$. Both measures are non-zero when $\frac{\tilde{\omega}}{\omega} \neq 1$ and grows significantly as the frequency quotient diverges from one. However, as $N_{\max}$ grows the interval where both measures are close to zero broadens.

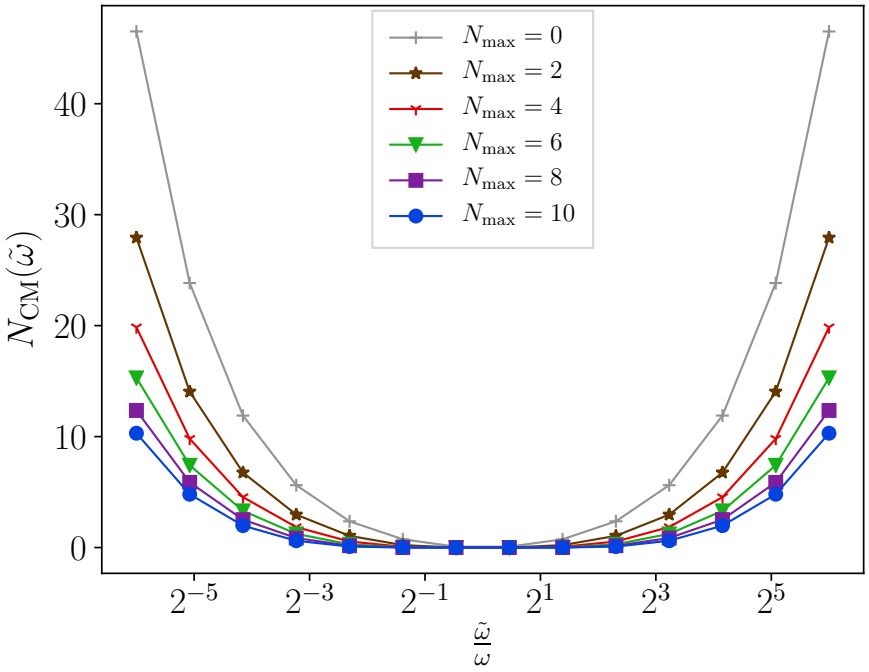

Figure 4.2: N_{CM} computed for the ground state of $H_{\text{HO}-\text{CM}}$ in a NCSM basis with frequency ω and truncation $N_{\max}$.

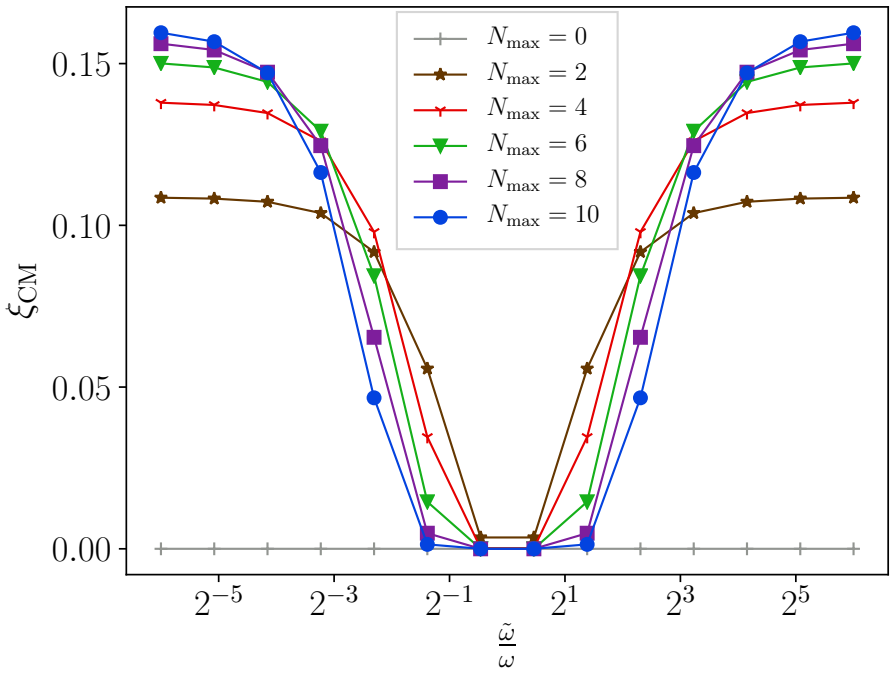

Figure 4.3: ξ_{CM} computed for the ground state of $H_{\mathrm{HO-CM}}$ in a NCSM basis with frequency ω and truncation $N_{\max}$.

The measures show a very different behaviour for large or small values of $\frac{\tilde{\omega}}{\omega}$. In the limits $\frac{\tilde{\omega}}{\omega} \to 0$ and $\frac{\tilde{\omega}}{\omega} \to \infty$ the metric N_{CM} grows to infinity. However, as seen in figure 4.3, ξ_{CM} grows to a finite value in the same limits. Since ξ_{CM} has a bounded growth pattern, unlike N_{CM}, it is a better choice when the estimated CM frequency, either $\tilde{\omega}_N$ or $\tilde{\omega}_\xi$, differs greatly from the basis frequency ω.

Chapter 5

Error analysis of NO2B

In chapter 3 I introduced the SR-NO2B-approximation of 3NFs in a HO-basis. I showed that it is able to capture the physics of 3NFs in ^{4}He for a NCSM basis with frequency $\hbar\omega = 20$ MeV and $N_{\max} \leq 10$. The fact that this particular choice of NCSM basis yields a good approximation of the 3NF could be just a coincidence. Is the approximation still valid when other frequencies are used?

Two complete HO bases with different frequencies span the same Hilbert space. For this reason, the results of two NCSM calculations using the same Hamiltonian, but at different frequencies, should converge to the same ground state as $N_{\max}$ increases.

The reference state used in the NO2B-approximation, introduced in chapter 3, depends on the basis frequency, $\hbar\omega$. Therefore, the NO2B-approximated 3NF depends on $\hbar\omega$ in a non-trivial way. Despite starting from the same Hamiltonian the NO2B-approximated Hamiltonian, H^{NO2B} will be different for each frequency. Therefore, the convergence property described in the previous paragraph, is not guaranteed for the NO2B-approximation.

In section 5.1 I will explore this possible frequency dependence of the approximation error. The ground-state energy of ^{4}He is computed for different basis frequencies with exact 3NF and with approximated ones. To see if the number of nucleons is important, the study is repeated for ^{16}O. For simplicity the SR-NO2B-approximation of 3NFs in a HO-basis will be referred to simply as the NO2B-approximation.

Part of an approximation error for the ground-state energy in the NO2B-approximation could potentially be explained by the translational symmetry breaking and CM-mixing, as discussed in chapter 4. In Section 5.2 I investigate the connection between the approximation error and the CM-mixing.

5.1 The $\hbar\omega$ dependence of NO2B results

The consequences of the frequency dependence of H^{NO2B} is explored in this section by comparing the ground-state energy for ^{4}He with exact 3NF and NO2B-approximated ones, computed with NCSM at different frequencies. To see if the frequency dependence is affected by the number of nucleons I also perform the same procedure for ^{16}O.

Figure 5.1 compares the ground-state energy, E_{gs}, of ^{4}He calculated for $\hbar\omega \in \{4, 8, \ldots, 32, 36\}$ MeV. The solid curves correspond to results ($E_{\mathrm{gs}}^{\mathrm{3NF}}$) with the full NNLO-sat interaction [17] including both 2NF and 3NF. The dashed curves are results ($E_{\mathrm{gs}}^{\mathrm{NO2B}}$) obtained with 2NF and NO2B-approximated 3NF.

As can be seen in figure 5.1, $E_{\mathrm{gs}}^{\mathrm{NO2B}}(N_{\mathrm{max}}, \hbar\omega) \approx E_{\mathrm{gs}}^{\mathrm{3NF}}$ for low frequencies, $\hbar\omega \leq 20$ MeV. There are only minor differences at these frequencies, $|E_{\mathrm{gs}}^{\mathrm{3NF}} - E_{\mathrm{gs}}^{\mathrm{NO2B}}| \equiv |\Delta E_{\mathrm{gs}}| \leq 1$ MeV. However, for $\hbar\omega > 20$ MeV the difference between $E_{\mathrm{gs}}^{\mathrm{NO2B}}$ and $E_{\mathrm{gs}}^{\mathrm{3NF}}$ gets increasingly larger with increasing HO frequency, $|\Delta E_{\mathrm{gs}}| \approx 8$ MeV for $\hbar\omega = 36$ MeV.

The difference, $E_{\mathrm{gs}}^{\mathrm{3NF}} - E_{\mathrm{gs}}^{\mathrm{NO2B}}$ is plotted in figure 5.2 as a function of $\hbar\omega$. The different curves correspond to $N_{\mathrm{max}} = 0$, 4, and 10.

The difference seems to increase with N_{max} for $\hbar\omega > 20$ MeV. At $N_{\mathrm{max}} = 0$ the difference between the full 3NF and NO2B is equal to zero, which is to expect since there is only one Slater determinant in the NCSM-basis, and it happens to be the reference state. There seems to exist a critical frequency, close to $\hbar\omega = 20$ MeV, where the difference is minimal for all model spaces.

It is now clear that the NO2B-approximated 3NF depends strongly on the basis frequency. I have demonstrated that this dependence strongly affects the ground-state energy in ^{4}He, but that there seems to exist a critical frequency where the difference between the NO2B-approximated 3NF and the exact one is very small. In the case studied here the critical frequency is close to 20 MeV, which explains why the benchmark presented in section 3.3 worked so well.

So far I have only looked at one, very small nucleus, ^{4}He, and observed a strong basis dependence in the NO2B-approximation error. Does this observation hold for other nuclei? The normal-ordering approximation is intended primarily for larger nuclei, where 3NFs are difficult to include exactly. In order to answer this question I have computed the ground-state energy for ^{16}O, both with an exact 3NF and an approximated one. In this case the NCSD code [36] has been used to perform the full 3NF-calculations.

The results of the ^{16}O calculations are shown in figure 5.3, as a function of $\hbar\omega$. The solid curves correspond to the NO2B-approximated 3NF, while the blue

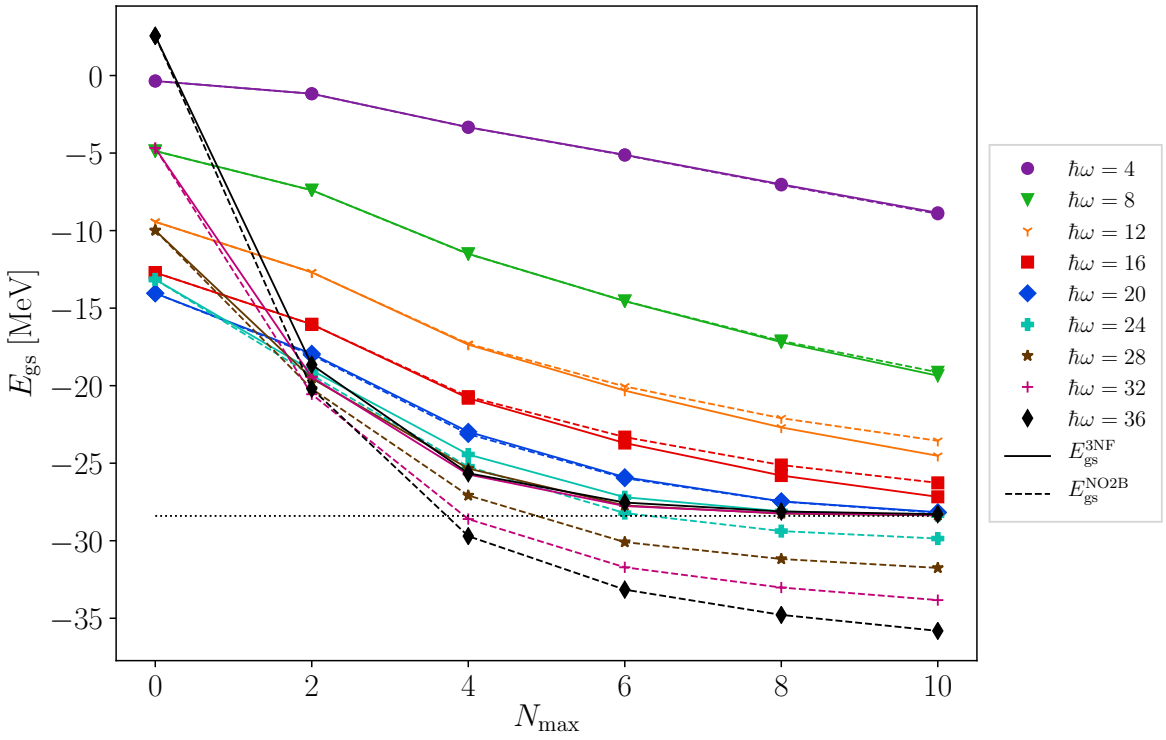

Figure 5.1: The ground-state energy of ^{4}He computed with the NNLO-sat interaction for different $\hbar\omega$. The solid lines are computed with 2NF and full inclusion of 3NF, while the dashed lines are computed with 2NF and NO2B-approximated 3NF. The dotted black line indicates the fully converged NNLO-sat ^{4}He [17]. Notice that while the full 3NF results seem to converge towards the same energy, the dotted line, the NO2B-approximated curves do not.

dotted circles corresponds to the full 3NF. Due to the extreme computational cost of including 3NFs in the NCSM for large A I have only been able to compute results with full 3NF up to $N_{\mathrm{max}} = 6$, and have limited the runs to four frequencies.

There is no visible difference between the binding-energy results with exact 3NF and the NO2B-approximated 3NF for the frequencies being studied. To illustrate this further, figure 5.4 shows the absolute difference between NO2B-approximated 3NFs and exact ones for the four frequencies where I have computed both of them. It is clear that the absolute difference is in the order of 1 MeV, which is much smaller than the absolute magnitude of the computed ground-state energies. These results suggest that the NO2B-approximation error for large nuclei such as ^{16}O is relatively

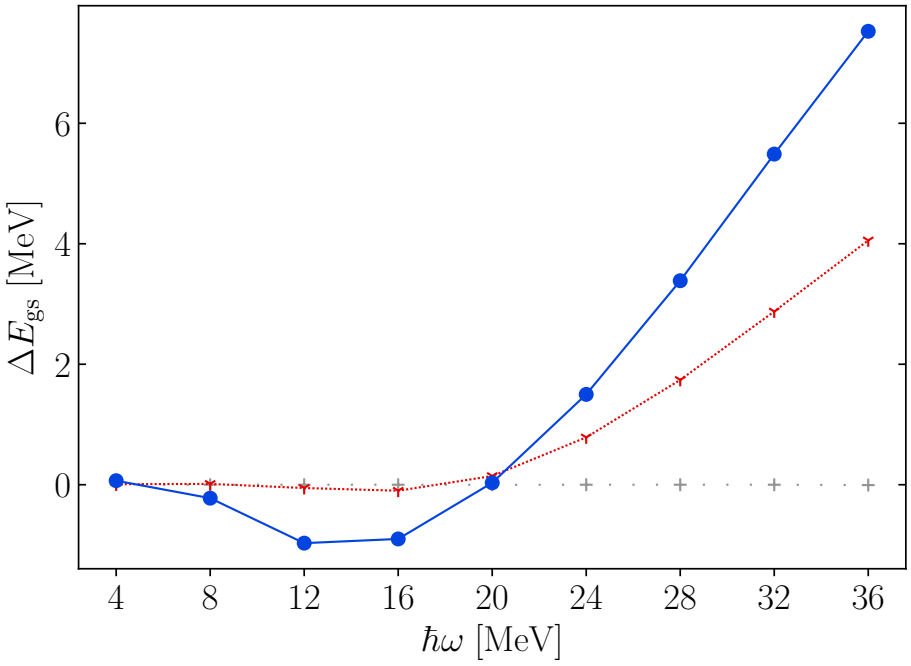

Figure 5.2: The difference between the NO2B-approximated ^{4}He-ground-state energy and the ^{4}He-ground-state energy computed with full inclusion of 3NF. The grey pluses are computed at $N_{\mathrm{max}} = 0$, the red y:s are computed at $N_{\mathrm{max}} = 4$ and the blue circles are computed at $N_{\mathrm{max}} = 10$.

small and does not depend strongly on the basis frequency.

That the difference between full the 3NF and NO2B-approximated one is not zero for $N_{\mathrm{max}} = 0$ is unexpected. However, it seems likely that this discrepancy comes from sligtly different definitions of fundamental constants, such as the nucleon masses, in the input to pAntoine and NCSD.

From the study above it is clear that the NO2B-approximation introduces an error with a strong dependence on $\hbar\omega$ in the ground-state energy for ^{4}He. However, the relative error is much smaller in ^{16}O suggesting that the larger the nucleus is the less of a problem this $\hbar\omega$ dependence becomes.

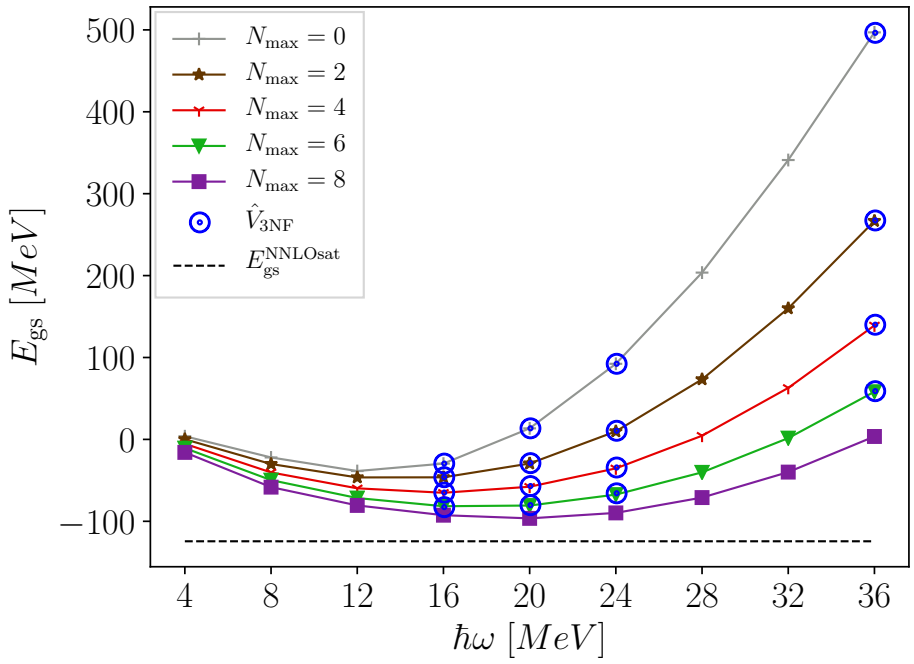

Figure 5.3: The ground-state energy of ^{16}O computed with NO2B-approximated 3NF (symbols connected with solid lines) and full inclusion of 3NF (open circles). The black dashed line is the ^{16}O NNLO-sat ground-state energy computed with CC [17].

5.2 The Center-of-Mass mixing from NO2B

The NO2B-approximation breaks the translational symmetry of the 3NF which can cause CM and intrinsic states to mix, as established in chapter 4. The failure of the NO2B-approximation to reproduce the ground-state energy of ^{4}He for some basis frequencies but works well for other, as seen in the previous section, could potentially be explained by this CM-mixing. Since the total mass of ^{16}O is larger than that of ^{4}He, exciting its CM requires more energy which could then explain why the approximation error is smaller for ^{16}O than for ^{4}He. In this section these two hypotheses are explored by computing the CM-mixing for the two nuclei when using the NO2B Hamiltonian.

The CM-mixing metrics, $\hbar\tilde{\omega}_N$ and $\hbar\tilde{\omega}_\xi$, of the ^{4}He ground-state with a NO2B-approximated 3NF are shown in figure 5.5. In the bottom panels the two CM-metrics,

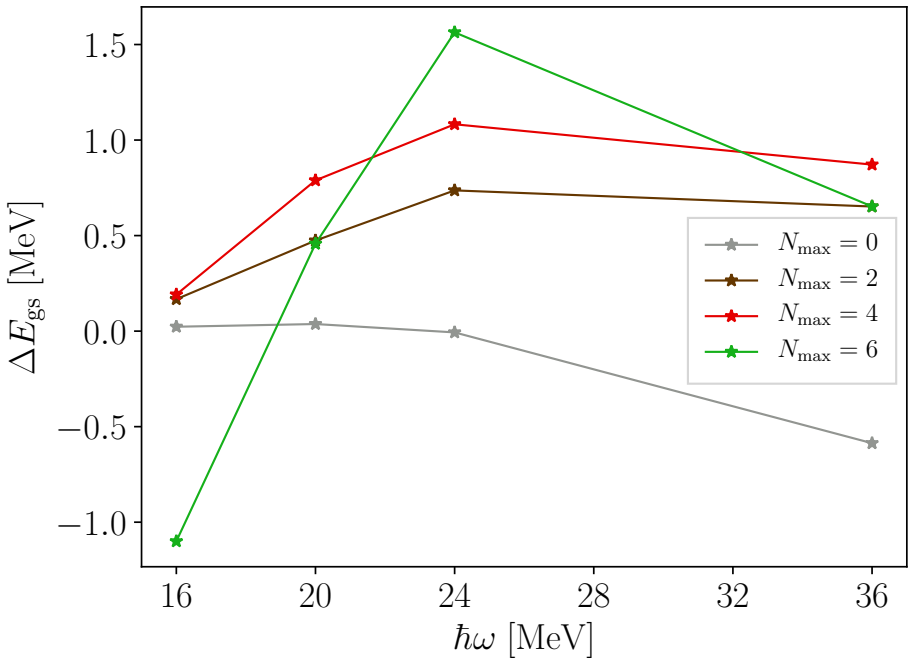

Figure 5.4: The difference in ground-state energy for ^{16}O between the NO2B-approximated 3NF and the exact one.

N_{CM} and ξ_{CM} are plotted with solid lines as functions of $\hbar\omega$. The CM-HO frequencies, $\hbar\tilde{\omega}_N$ and $\hbar\tilde{\omega}_\xi$, are plotted in the two top panels. I have added a dashed curve in the lower left panel illustrating what N_{CM} would be if the CM-part really is a HO-ground state with frequency $\hbar\tilde{\omega}_N$. It is computed for the ground state of the Hamiltonian in equation (4.24) for $\tilde{\omega} = \tilde{\omega}_N$, in accordance with the second limitation in section 4.3.3.

The solid curve in the (lower left) N_{CM} panel is close to zero for basis frequencies less than 20 MeV, and grows to 0.6 for larger frequencies. Since the solid curve differs from the dashed one this growth can not be explained by representing a HO-ground state with frequency $\hbar\tilde{\omega}_N$ in a NCSM basis with frequency $\hbar\omega$. Instead, this difference between the solid and dashed curves indicates strong CM-mixing.

The two different CM-metrics, N_{CM} and ξ_{CM}, show a very similar behaviour. Both are very low for $\hbar\omega \leq 20$ MeV but increase significantly for higher frequencies. In the previous section, the frequency $\hbar\omega = 20$ MeV turned out to be critical, where the NO2B-approximation error is positive above this frequency and negative below it.

Furthermore, for basis frequencies below (above) this critical value the approximation error was relatively small (very large). Since the N_{CM} and ξ_{CM} metrics are large above 20 MeV, it seems as if an NO2B-induced attractive energy contribution comes from CM-excitations in this region. The repulsive error, however, remains unexplained. I can speculate that its origin is the neglected $\hat{W}^{3b}_{\text{3nf}}$ term.

In figure 5.6, the CM-mixing metrics for ^{16}O with a NO2B-approximated 3NF is plotted as a function of basis frequency. The figure is organized in the same way as figure 5.5 for ^{4}He.

In this case, the size of the N_{CM} and ξ_{CM} metrics are between one and two orders of magnitude smaller compared to their ^{4}He counterparts. Furthermore, the extracted frequencies, $\hbar\tilde{\omega}_N$ and $\hbar\tilde{\omega}_\xi$, are very close to the basis frequency. Therefore, it seems as the CM-mixing is much smaller in ^{16}O than in ^{4}He. As seen in the previous section, the absolute difference between the ^{16}O ground-state energy computed with NO2B-approximated 3NFs and with exact ones is very small. Because of these three observations, the NO2B-approximation seems to capture most of the physics of the 3NF in ^{16}O.

Since the NO2B-approximation is more relevant for larger nuclei than ^{4}He this last observation is promising. The fact that the CM-mixing is low for large nuclei over a large range of frequencies means that it can be used with some confidence in conjunction with, for instance, NCSM extrapolation methods as was briefly discussed in section 2.1.

Before, ending this chapter I want to give a word of caution concerning convergence. While the ^{4}He results are close to fully converged, the ^{16}O ones are not. For both nuclei the general trend is that the CM-mixing metrics increases with N_{max}. Therefore, it is not unreasonable to assume that this trend continues beyond $N_{\text{max}} = 8$ for ^{16}O, that has been the computational limit in this study. It could therefore be the case that a stronger CM-mixing might emerge if the ^{16}O calculations were to be performed in larger NCSM bases. For this reason I strongly recommend to check that the CM-mixing is small before trusting any NCSM result with a SR-NO2B-approximated 3NF in a HO basis. In fact, this caution of checking CM-mixing can be seen as a general recommendation when using a Hamiltonian or many-body method that breaks the translational symmetry.

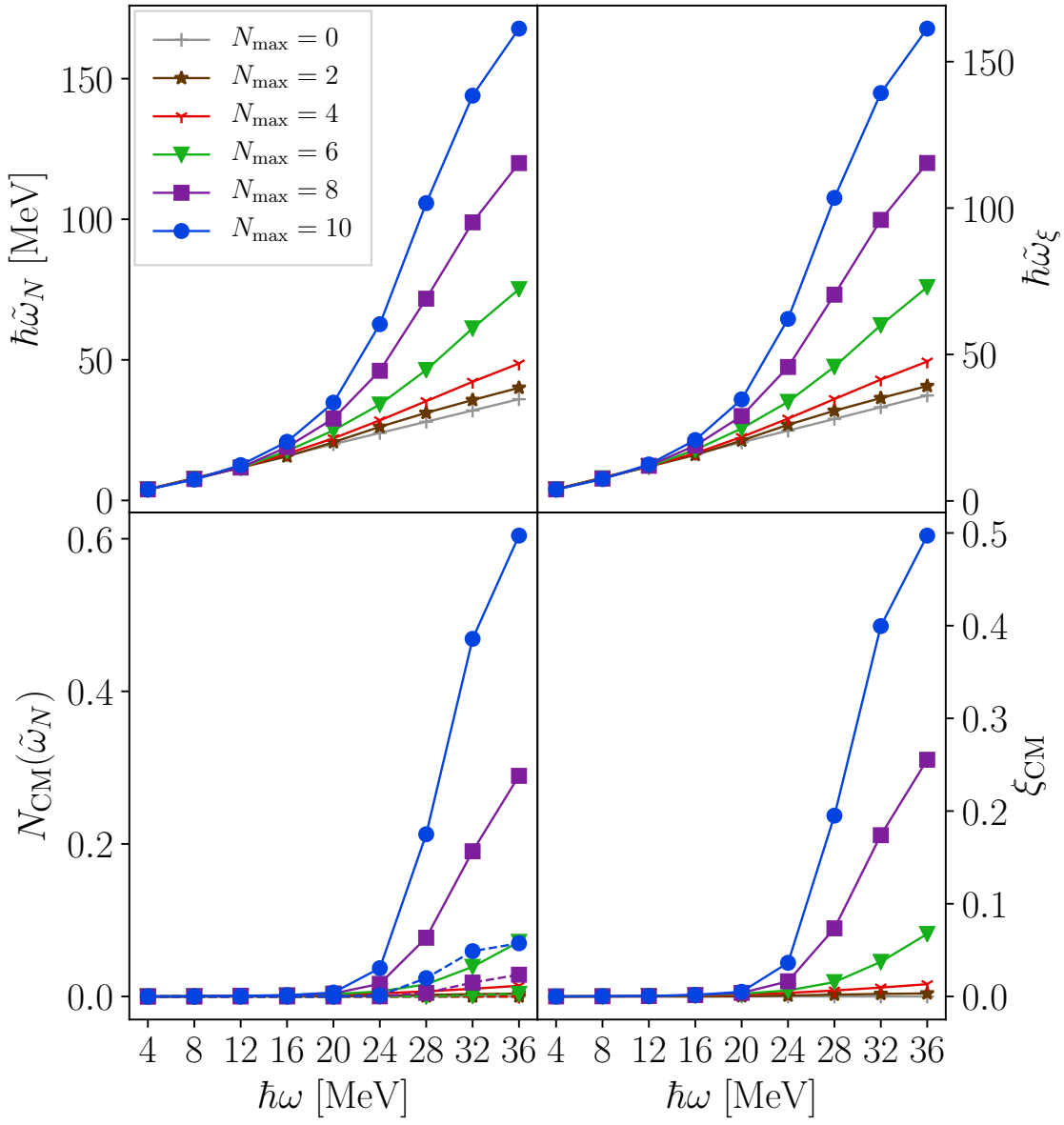

Figure 5.5: The two CM-metrics, introduced in section 4.3, computed for ^{4}He with a NO2B-approximated 3NF. The upper panels display the CM HO-frequencies $\hbar\tilde{\omega}_N$ and $\hbar\tilde{\omega}_\xi$, respectively, and the lower panels contain the measures $\hbar\tilde{\omega}_N$ and $\hbar\tilde{\omega}_\xi$. The dashed curve in the lower left panel indicates what N_{CM} would be if the CM-part of the ground state really was a HO-ground state with frequency $\hbar\tilde{\omega}_N$.

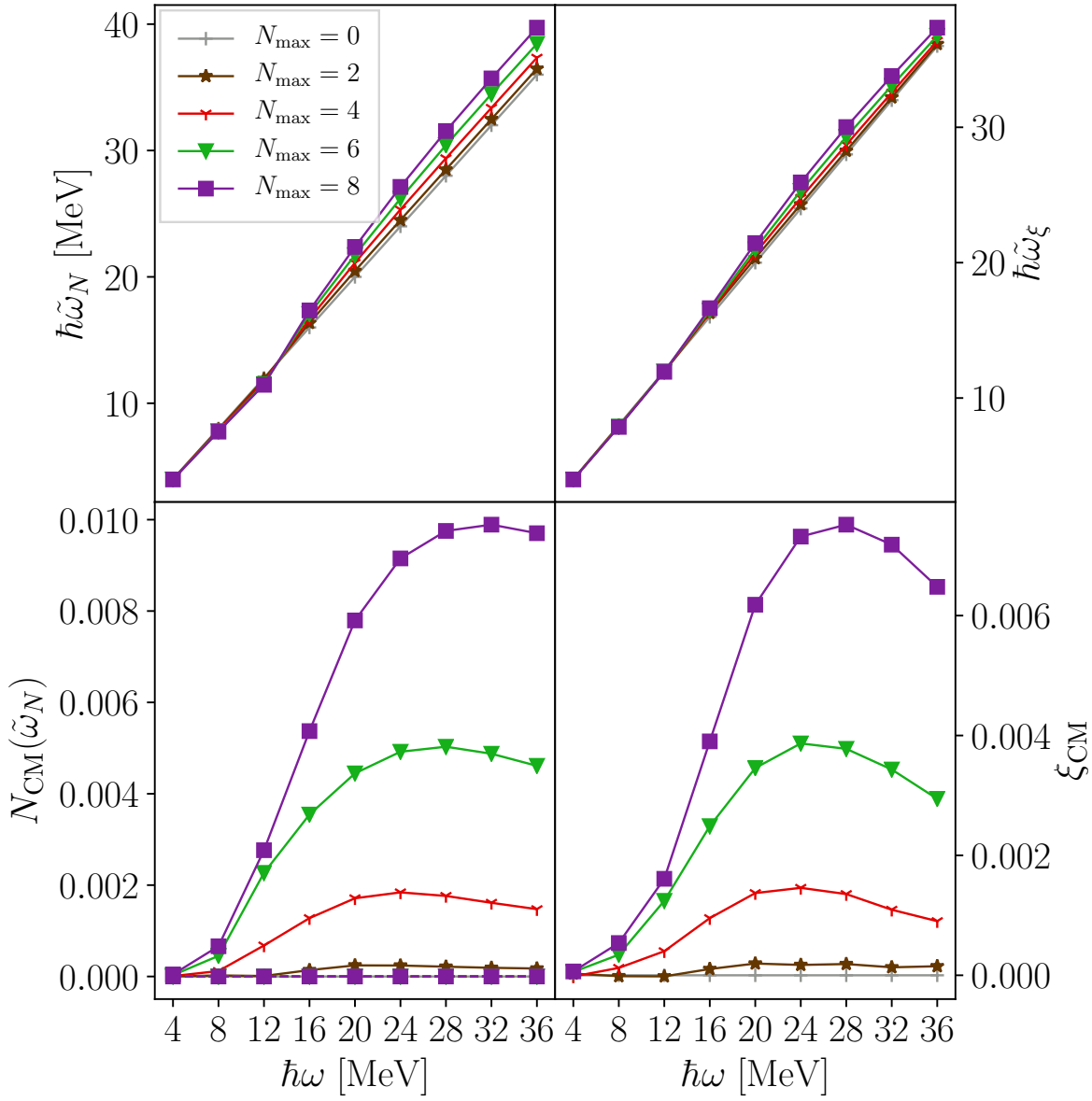

Figure 5.6: The two CM-metrics, introduced in section 4.3, computed for ^{16}O with a NO2B-approximated 3NF. The upper panels display the CM HO-frequencies, $\hbar\tilde{\omega}_N$ and $\hbar\tilde{\omega}_\xi$, respectively, and the lower panels contain the measures N_{CM} and ξ_{CM}. The dashed curves in the lower left panel indicates what N_{CM} would be if the CM-part of the ground state really was a HO-ground state with frequency $\hbar\tilde{\omega}_N$. Note that the dashed curves are all zero.

Chapter 6

Discussion and outlook

The purpose of this work was to contribute to the understanding of how atomic nuclei emerge from the fundamental forces of nature, i.e. the *ab initio* approach to nuclear structure. At a fundamental level the strong nuclear force is described by QCD. However, at the low momentum scale of atomic nuclei it is non-perturbative and χEFTs should provide a more practical description. χEFTs predict the existence of many-nucleon forces and it is not possible to get rid of them. Due to combinatorial reasons, many-nucleon forces are computationally demanding and require rapidly increasing computational resources the more particles they involve. For this reason, most nuclear calculations have only included 2NFs. However, for the last two decades calculations including 3NFs have become more common.

The dynamics of a many-body quantum system, such as the atomic nucleus, is governed by the MBSE. To solve the MBSE, in this work, the NCSM has been employed. In this *ab initio* method all the nucleons are dynamical particles. The MBSE is expanded in a finite HO many-body basis truncated on the total HO excitation energy, yielding a finite matrix eigenvalue problem. With this basis truncation, the NCSM eigenstates separate in CM and intrinsic parts, given that the Hamiltonian is translationally symmetric. This makes it possible to study the internal dynamics of the nucleus without having to worry about spurious CM-mixing.

In the NCSM, 3NFs are straightforward to implement but they make simulations extremely computationally demanding. Therefore, an approximation scheme is called for. In this work a version of the NO2B-approximation, described in chapter 3, has been evaluated for use in the NCSM. The reference state is chosen to be a Slater determinant constructed from HO-states. This choice of reference state makes the implementation of the NO2B-approximation relatively simple, although it limits the method to closed-core nuclei.

In section 4.2, I showed that the NO2B-approximation breaks the translational symmetry of the 3NF, since the frame of reference is fixed by the reference state. This has the consequence that the energy eigenstates, computed by the NCSM, are no longer guaranteed to separate CM-motion from internal-dynamics. Two diagnostics, N_{CM} and ξ_{CM} were introduced in section 4.3, in order to study the effect of CM-mixing.

Physical observables should not depend on the choice of the NCSM-basis. However, the NO2B-approximation introduces a basis dependence in the approximate 3NFs. The consequence of this basis dependence was investigated in section 5.1. The frequency, $\hbar\omega$, of the basis was varied while the ground-state energies of ^{4}He and ^{16}O was computed with a NO2B-approximated 3NF and then compared to corresponding values with exact inclusion of 3NFs.

As was presented in figure 5.1 the NO2B-approximated ground-state energy of ^{4}He depends strongly on the basis frequency. For frequencies below 20 MeV the NO2B-approximation underbinds the nucleus. However, the approximated 3NF deviated less than 1 MeV from full 3NF for these basis frequencies. For frequencies above 20 MeV, the approximated 3NF overbinds the nucleus, with a large deviation of several MeV. The smallest approximation error is observed at $\hbar\omega = 20$ MeV.

In section 5.2, I investigated if the CM-problem can explain the frequency dependence of the NO2B-approximated ^{4}He ground-state energy. In figure 5.5 the two metrics, N_{CM} and ξ_{CM}, computed for ^{4}He with a NO2B-approximated 3NF was plotted. This figure showed that there were almost no CM-mixing for basis frequencies less than 20 MeV, while for larger frequencies there were significant CM-mixing in the ground-state. This could likely explain the observed change in behaviour of the ground-state energy at $\hbar\omega = 20$ MeV. There seem to be two competing approximation errors, one that is due to the CM-mixing and is strongly attractive and a different one, from the discarded three-nucleon potential, that is weakly repulsive. Exact mechanism for the second error is currently unknown. At the frequency 20 MeV these two errors cancel each other and therefore gives an apparent good approximation.

When ^{16}O was subjected to the same investigation, I observed that the NO2B-approximated ground-state energy, figure 5.3, has a very small approximation error. The difference in ground-state energy between the approximated 3NF and the exact one was found to be very small. The absolute error in energy was on the order of 1 MeV which corresponds to a relative error of $\lesssim 1$ MeV. The CM-mixing in ^{16}O was shown in figure 5.6, to be almost two orders of magnitude smaller than the corresponding ^{4}He values. This suggests that the CM-mixing might be less of a problem for heavier nuclei. This result is not entirely unexpected. Because of the

larger total mass of the system, it requires more energy, than for light nuclei, to excite the CM-degree of freedom.

The ^{4}He results were relatively close to fully converged NCSM results. Therefore, the strong basis dependence of the NO2B-approximated ^{4}He ground-state is quite certain. However, the ^{16}O results were far from fully converged. The CM-mixing of ^{16}O, while low, is in fact growing with increasing $N_{\max}$. Therefore, it is not certain that CM-mixing remains low in the limit of converged results. Because of this observation I issue a decree of caution, to always observe the CM-mixing before trusting any results computed with SR-NO2B-approximated 3NF in a HO-basis.

To mitigate the problems, discussed above, it could be preferable to carry out the NO2B-approximation in a different basis [37]. As a prelude to the discussion about the continuation of this project, I will briefly discuss benefits and downsides of alternatives to formulating the SR-NO2B-approximation in a HO-basis.

An alternative choice of reference state in the SR-NO2B-approximation is to choose the Hartree-Fock (HF) state for the nucleus of interest. The HF state is a Slater-determinant constructed from a single particle basis in such a way that it approximates the energy-ground state through the variational principle. The HF state is independent of the basis, the HO frequency dependence that we have observed in this work would probably not emerge to the same extent if a HF-state was used as a reference state.

The use of a HF-state as a reference state would not get rid of the CM-mixing entirely, for two reasons. The first reason is that this too would fixate the frame of reference and thus induce explicit translational symmetry breaking in the Hamiltonian. Secondly, the truncation of the HO-basis used in the HF-method is on the single-particle energy, while in the NCSM it is on the total HO-energy. Therefore, the NCSM can not guarantee a separation between CM- and intrinsic excitations in the ground state. However, HF-normal-ordered Hamiltonians have been used without inducing large CM-mixing in other methods, such as the CC-method [34], therefore, this might not be a big problem.

A different alternative could be to use a NCSM-ground state for a smaller $N_{\max}$ as reference state. In this case the application of the MR-NO2B-approximation would be required. In the MR-NO2B-approximation, a general many-body state, consisting of many Slater determinants, is used as a reference state. An obvious advantage is that the MR-NO2B-approximation is not limited to closed-core systems and can be applied to many different nuclei. However, there are a few modifications to the NO2B-approximation that would be necessary to be able to use MR-NO2B. For instance, it would be required to introduce many-body contractions on top of the single-particle ones discussed in section 3.1.1. Therefore, it would not be possible to

use the code that I have already developed for SR-NO2B.

The MR-NO2B-approximation does not eliminate the CM-mixing problem. Just as the other methods any choice of reference state would fix the frame of reference and thus explicitly break the translational symmetry. Therefore, I suggest that CM-mixing should always be measured when a NO2B-approximation, of any kind, is used.

Since the NO2B-approximation could be useful for the study of larger nuclei, increasing the capabilities of the cNO2B program could be of future interest. For instance, currently cNO2B needs the 3NFs in M-scheme format. Rewriting the code to use J-scheme elements directly would make it possible to use it in larger model spaces.

Because of the limitations to the NO2B-approximation discussed above, it is clear that the use of exact 3NFs is preferable for light nuclei, $A < 16$. For this reason, a natural next step is to develop a NCSM-code with the capabilities to use both 2NF and full-3NF.

Bibliography

[1] Dr. H. Geiger and E. Marsden. "LXI. The laws of deflexion of a particles through large angles". In: *The London, Edinburgh, and Dublin Philosophical Magazine and Journal of Science* 25.148 (1913), pp. 604–623. DOI: 10.1080/14786440408634197. eprint: https://doi.org/10.1080/14786440408634197. URL: https://doi.org/10.1080/14786440408634197.

[2] Hans-Werner Hammer, Andreas Nogga and Achim Schwenk. "Colloquium: Three-body forces: From cold atoms to nuclei". In: *Rev. Mod. Phys.* 85 (1 2013), pp. 197–217. DOI: 10.1103/RevModPhys.85.197. URL: https://link.aps.org/doi/10.1103/RevModPhys.85.197.

[3] Frank Winter et al. "First lattice QCD study of the gluonic structure of light nuclei". In: *Phys. Rev. D* 96 (9 2017), p. 094512. DOI: 10.1103/PhysRevD.96.094512. URL: https://link.aps.org/doi/10.1103/PhysRevD.96.094512.

[4] D. Dubbers et al. "Exotic decay channels are not the cause of the neutron lifetime anomaly". In: *Physics Letters B* 791 (2019), pp. 6 –10. ISSN: 0370-2693. DOI: https://doi.org/10.1016/j.physletb.2019.02.013. URL: http://www.sciencedirect.com/science/article/pii/S0370269319301066.

[5] Steven Weinberg. "Phenomenological Lagrangians". In: *Physica A: Statistical Mechanics and its Applications* 96.1 (1979), pp. 327 –340. ISSN: 0378-4371. DOI: https://doi.org/10.1016/0378-4371(79)90223-1. URL: http://www.sciencedirect.com/science/article/pii/0378437179902231.

[6] R. Machleidt and D.R. Entem. "Chiral effective field theory and nuclear forces". In: *Physics Reports* 503.1 (2011), pp. 1 –75. ISSN: 0370-1573. DOI: https://doi.org/10.1016/j.physrep.2011.02.001. URL: http://www.sciencedirect.com/science/article/pii/S0370157311000457.

[7] Evgeny Epelbaum. "Nuclear Forces from Chiral Effective Field Theory: A Primer". In: 2010. arXiv: 1001.3229 [nucl-th].

[8] Bruce R. Barrett, Petr Navrátil and James P. Vary. "Ab initio no core shell model". In: *Progress in Particle and Nuclear Physics* 69 (2013), pp. 131 – 181. ISSN: 0146-6410. DOI: https://doi.org/10.1016/j.ppnp.2012.10.003. URL: http://www.sciencedirect.com/science/article/pii/S0146641012001184.

[9] B. S. Pudliner et al. "Quantum Monte Carlo calculations of nuclei with $A \leq 7$". In: *Phys. Rev. C* 56 (4 1997), pp. 1720–1750. DOI: 10.1103/PhysRevC.56.1720. URL: https://link.aps.org/doi/10.1103/PhysRevC.56.1720.

[10] D. J. Dean and M. Hjorth-Jensen. "Coupled-cluster approach to nuclear physics". In: *Phys. Rev. C* 69 (5 2004), p. 054320. DOI: 10.1103/PhysRevC.69.054320. URL: https://link.aps.org/doi/10.1103/PhysRevC.69.054320.

[11] Alexander Tichai et al. "Hartree–Fock many-body perturbation theory for nuclear ground-states". In: *Physics Letters B* 756 (2016), pp. 283 –288. ISSN: 0370-2693. DOI: https://doi.org/10.1016/j.physletb.2016.03.029. URL: http://www.sciencedirect.com/science/article/pii/S0370269316002008.

[12] David C. J. Marsden et al. "Feasibility study of a three-nucleon force in the no-core shell model: ^{3}H binding energy". In: *Phys. Rev. C* 66 (4 2002), p. 044007. DOI: 10.1103/PhysRevC.66.044007. URL: https://link.aps.org/doi/10.1103/PhysRevC.66.044007.

[13] Sven Binder et al. "Ab initio calculations of medium-mass nuclei with explicit chiral $3N$ interactions". In: *Phys. Rev. C* 87 (2 2013), p. 021303. DOI: 10.1103/PhysRevC.87.021303. URL: https://link.aps.org/doi/10.1103/PhysRevC.87.021303.

[14] Robert Roth et al. "Medium-Mass Nuclei with Normal-Ordered Chiral NN+$3N$ Interactions". In: *Phys. Rev. Lett.* 109 (5 2012), p. 052501. DOI: 10.1103/PhysRevLett.109.052501. URL: https://link.aps.org/doi/10.1103/PhysRevLett.109.052501.

[15] Eskendr Gebrerufael, Angelo Calci and Robert Roth. "Open-shell nuclei and excited states from multireference normal-ordered Hamiltonians". In: *Phys. Rev. C* 93 (3 2016), p. 031301. DOI: 10.1103/PhysRevC.93.031301. URL: https://link.aps.org/doi/10.1103/PhysRevC.93.031301.

[16] Bruce R. Barrett, Petr Navrátil and James P. Vary. "Ab initio no core shell model". In: *Progress in Particle and Nuclear Physics* 69 (2013), pp. 131 – 181. ISSN: 0146-6410. DOI: https://doi.org/10.1016/j.ppnp.2012.10.003. URL: http://www.sciencedirect.com/science/article/pii/S0146641012001184.

[17] A. Ekström et al. "Accurate nuclear radii and binding energies from a chiral interaction". In: *Phys. Rev. C* 91 (5 2015), p. 051301. DOI: 10.1103/PhysRevC.91.051301. URL: https://link.aps.org/doi/10.1103/PhysRevC.91.051301.

[18] C. Forssén et al. "Converging sequences in the ab initio no-core shell model". In: *Phys. Rev. C* 77 (2 2008), p. 024301. DOI: 10.1103/PhysRevC.77.024301. URL: https://link.aps.org/doi/10.1103/PhysRevC.77.024301.

[19] H. Zhan et al. "Extrapolation method for the no-core shell model". In: *Phys. Rev. C* 69 (3 2004), p. 034302. DOI: 10.1103/PhysRevC.69.034302. URL: https://link.aps.org/doi/10.1103/PhysRevC.69.034302.

[20] S.K. Bogner et al. "Convergence in the no-core shell model with low-momentum two-nucleon interactions". In: *Nuclear Physics A* 801.1 (2008), pp. 21 –42. ISSN: 0375-9474. DOI: https://doi.org/10.1016/j.nuclphysa.2007.12.008. URL: http://www.sciencedirect.com/science/article/pii/S0375947407008147.

[21] K. A. Wendt et al. "Infrared length scale and extrapolations for the no-core shell model". In: *Phys. Rev. C* 91 (6 2015), p. 061301. DOI: 10.1103/PhysRevC.91.061301. URL: https://link.aps.org/doi/10.1103/PhysRevC.91.061301.

[22] James P Vary et al. "Ab initionuclear structure – the large sparse matrix eigenvalue problem". In: *Journal of Physics: Conference Series* 180 (2009), p. 012083. DOI: 10.1088/1742-6596/180/1/012083. URL: https://doi.org/10.1088%2F1742-6596%2F180%2F1%2F012083.

[23] P. Sternberg et al. "Accelerating configuration interaction calculations for nuclear structure". In: *SC '08: Proceedings of the 2008 ACM/IEEE Conference on Supercomputing*. 2008, pp. 1–12. DOI: 10.1109/SC.2008.5220090.

[24] C. Forssén et al. "Large-scale exact diagonalizations reveal low-momentum scales of nuclei". In: *Phys. Rev. C* 97 (3 2018), p. 034328. DOI: 10.1103/PhysRevC.97.034328. URL: https://link.aps.org/doi/10.1103/PhysRevC.97.034328.

[25] E. Caurier et al. "The shell model as a unified view of nuclear structure". In: *Rev. Mod. Phys.* 77 (2 2005), pp. 427–488. DOI: 10.1103/RevModPhys.77.427. URL: https://link.aps.org/doi/10.1103/RevModPhys.77.427.

[26] W.H.Dickhoff and D.Van Neck. *Many-Body theory exposed! Propagator Description of Quantum Mechanics*. 2nd ed. Vol. 1. 5 Toh Tuck Link, Singapore 596224: World Scientific Publishing Co. Pte. Ltd., 2008. ISBN: 13 978-981-281-379-4.

[27] A. Ekström et al. "Optimized Chiral Nucleon-Nucleon Interaction at Next-to-Next-to-Leading Order". In: *Phys. Rev. Lett.* 110 (19 2013), p. 192502. DOI: 10.1103/PhysRevLett.110.192502. URL: https://link.aps.org/doi/10.1103/PhysRevLett.110.192502.

[28] P. Navrátil, G. P. Kamuntavičius and B. R. Barrett. "Few-nucleon systems in a translationally invariant harmonic oscillator basis". In: *Phys. Rev. C* 61 (4 2000), p. 044001. DOI: 10.1103/PhysRevC.61.044001. URL: https://link.aps.org/doi/10.1103/PhysRevC.61.044001.

[29] Dag Fahlin Strömberg. "Three-Nucleon Forces Through Normal-Ordered Approximations". 44. MA thesis. 2016.

[30] Tor Djärv. "Three-Body Forces in Configuration-Interaction Methods for Nuclear Physics". 48. MA thesis. 2016.

[31] Joachim Langhammer. "Chiral Three-Nucleon Interactions in Ab-Initio Nuclear Structure and Reactions". PhD thesis. Darmstadt: Technische Universität, 2014. URL: http://tuprints.ulb.tu-darmstadt.de/3945/.

[32] R.D Lawson. *Theory of the nuclear shell model*. Clarendon, 1980.

[33] Nielsen M.A and Chuang I.L. *Quantum computation and quantum information*. 10th ed. Vol. 1. Cambridge university press, 2010. ISBN: 978-1-107-00217-3.

[34] G. Hagen, T. Papenbrock and D. J. Dean. "Solution of the Center-Of-Mass Problem in Nuclear Structure Calculations". In: *Phys. Rev. Lett.* 103 (6 2009), p. 062503. DOI: 10.1103/PhysRevLett.103.062503. URL: https://link.aps.org/doi/10.1103/PhysRevLett.103.062503.

[35] N. M. Parzuchowski et al. "Ab initio electromagnetic observables with the in-medium similarity renormalization group". In: *Phys. Rev. C* 96 (3 2017), p. 034324. DOI: 10.1103/PhysRevC.96.034324. URL: https://link.aps.org/doi/10.1103/PhysRevC.96.034324.

[36] Navratil P. "No-core shell model slater determinant code (NCSD) Unpublished". In: (2011).

[37] Alexander Tichai et al. "Natural orbitals for ab initio no-core shell model calculations". In: *Phys. Rev. C* 99 (3 2019), p. 034321. DOI: 10.1103/PhysRevC.99.034321. URL: https://link.aps.org/doi/10.1103/PhysRevC.99.034321.

Appendix A

When can N_{CM} and ξ_{CM} show Center-of-Mass separation?

In section 4.3 I introduced two metrics: N_{CM} and ξ_{CM}, to measure to what degree the NCSM state, computed with NO2B-approximated 3NFs, separates the CM and intrinsic dynamics. However, the two metrics can not do so in every situation. In this appendix one such situation is explored in detail.

Idealy I want to be able to distinguish the two situations:

a) The CM-state is a pure quantum state

$$|\Psi_{\mathrm{gs-CM}}\rangle = \sum_{\mathcal{N},\mathcal{L}} \phi_{\mathcal{N},\mathcal{L}} \, |\mathcal{N},\mathcal{L}\rangle \, . \tag{A.1}$$

b) The CM-state is a mixed quantum state and must be represented by a density matrix

$$\hat{\rho}_{\mathrm{CM}} = \sum_{\substack{\mathcal{N},\mathcal{L} \\ \mathcal{N}',\mathcal{L}'}} \rho_{\mathcal{N},\mathcal{L},\mathcal{N}',\mathcal{L}'} \, |\mathcal{N},\mathcal{L}\rangle \, \langle \mathcal{N}',\mathcal{L}'| \, . \tag{A.2}$$

In both a) and b) $|\mathcal{N},\mathcal{L}\rangle$ where $\mathcal{N}$, $\mathcal{L} \geq 0$ are HO eigenstates in the CM-coordinate for the optimal frequency $\tilde{\omega}$. I note that case a) is a special case of b) where $\rho_{\mathcal{N},\mathcal{L},\mathcal{N}',\mathcal{L}'} = \phi_{\mathcal{N},\mathcal{L}} \phi_{\mathcal{N}',\mathcal{L}'}$.

I compute the N_{CM} metric in both cases and obtain

a)

$$N_{\mathrm{CM}} = \sum_{\mathcal{N},\mathcal{L}} |\phi_{\mathcal{N},\mathcal{L}}|^2 \, (2\mathcal{N} + \mathcal{L}) \tag{A.3}$$

b)

$$N_{\mathrm{CM}} = \sum_{\mathcal{N},\mathcal{L}} \rho_{\mathcal{N},\mathcal{L},\mathcal{N},\mathcal{L}}(2\mathcal{N}+\mathcal{L}) \tag{A.4}$$

The coefficients $|\phi_{\mathcal{N},\mathcal{L}}|^2 \geq 0$ for all $\mathcal{N},\mathcal{L}$. If I assume that not only $|\phi_{0,0}|^2 > 0$ then $N_{\mathrm{CM}} > 0$. The coefficients $\rho_{\mathcal{N},\mathcal{L},\mathcal{N},\mathcal{L}}$ must also be larger than or equal to zero. This can be seen by relating equation (A.2) with equation (4.13) yielding the equation

$$\rho_{\mathcal{N},\mathcal{L},\mathcal{N},\mathcal{L}} = \sum_i c_{i,j} c^*_{i,j} = \sum_i |c_{i,j}|^2 \tag{A.5}$$

assuming that $|\mathcal{N},\mathcal{L}\rangle = \left|\Psi^j_{\mathrm{CM}}\right\rangle$. Therefore, it follows that $N_{\mathrm{CM}} > 0$ for case b) unless only $\rho_{0,0,0,0}$ is non-zero. This proves the first part of the statement, that $N_{\mathrm{CM}} = 0$ implies that $|\Psi_{\mathrm{gs-CM}}\rangle$ is a HO-ground state.

The equations (A.3) and (A.4) are indistinguishable in the sense that given a value of $N_{\mathrm{CM}} > 0$ it is impossible to determine which case it is. Therefore, the second part of the statement, that N_{CM} can not distinguish between a general separable ground state and a general entangled ground state, is proven for N_{CM}.

Let us turn to the ξ_{CM} metric. To simplify the calculation of ξ_{CM} in both cases I introduce the quantities A and B such that

a)

$$A = \sum_{\mathcal{N},\mathcal{L}} |\phi_{\mathcal{N},\mathcal{L}}|^2 \left(2\mathcal{N}+\mathcal{L}+\frac{3}{2}\right) \tag{A.6}$$

$$B = \sum_{\mathcal{N},\mathcal{L}} \sqrt{(\mathcal{N}+1)\left(\mathcal{N}+\mathcal{L}+\frac{3}{2}\right)} \left(\phi^*_{\mathcal{N},\mathcal{L}}\phi_{\mathcal{N}+1,\mathcal{L}} + \phi^*_{\mathcal{N}+1,\mathcal{L}}\phi_{\mathcal{N},\mathcal{L}}\right) \tag{A.7}$$

b)

$$A = \sum_{\mathcal{N},\mathcal{L}} \rho_{\mathcal{N},\mathcal{L},\mathcal{N},\mathcal{L}} \left(2\mathcal{N}+\mathcal{L}+\frac{3}{2}\right) \tag{A.8}$$

$$B = \sum_{\mathcal{N},\mathcal{L}} \sqrt{(\mathcal{N}+1)\left(\mathcal{N}+\mathcal{L}+\frac{3}{2}\right)} \left(\rho_{\mathcal{N},\mathcal{L},\mathcal{N}+1,\mathcal{L}} + \rho_{\mathcal{N}+1,\mathcal{L},\mathcal{N},\mathcal{L}}\right) \tag{A.9}$$

In both a) and b) the expectation values of $\hat{R}^2_{\mathrm{CM}}$ and $\hat{P}^2_{\mathrm{CM}}$ can be written as

$$\langle \hat{R}^2_{\mathrm{CM}} \rangle = b^2 (A - B) \tag{A.10}$$

$$\langle \hat{P}^2_{\mathrm{CM}} \rangle = \frac{\hbar^2}{b^2} (A + B) \tag{A.11}$$

which gives that

$$\xi_{\mathrm{CM}} = \sqrt{A^2 - B^2} - \frac{3}{2}. \tag{A.12}$$

Given a value of $\xi_{\mathrm{CM}} > 0$ it is clear that either case, a) or b), could have been the starting point. Therefore, ξ_{CM} can not distinguish a) from b) if $\xi_{\mathrm{CM}} > 0$.[1]

It is now clear that a separation can only be conclusively when $|\Psi_{\mathrm{CM}}\rangle$ is a HO-ground state since this is the only case when both measurs are zero. In all other cases, both N_{CM} and ξ_{CM} are greater than zero and CM-separation is indistinguishable from CM-mixing.

[1]That $\xi_{\mathrm{CM}} = 0$ implies that the CM state is a HO ground state is not clear from this. It is not obvious that there does not exists some exotic state forwhich $B^2 > 0$ and $B^2 = A^2$. Therefore, I have decided to not investigate this in the scope of this project.

Appendix B

Useful proofs

In this appendix chapter I prove some usefull statements. Any quantumstate used in the proofs are assumed to be normalized.

B.1 Proof that the ξ_{CM} measure is positive

In section 4.3.2 I introduced the quantity ξ_{CM} as

$$\xi_{\mathrm{CM}} = \frac{\sqrt{\langle \hat{P}^2_{\mathrm{CM}} \rangle \langle \hat{R}^2_{\mathrm{CM}} \rangle}}{\hbar} - \frac{3}{2}. \tag{B.1}$$

In this section I will prove that $\xi_{\mathrm{CM}} \geq 0$.

Let us focus on the nominator in equation B.1,

$$\sqrt{\langle \hat{P}_{\mathrm{CM}} \rangle \langle \hat{R}_{\mathrm{CM}} \rangle}. \tag{B.2}$$

This quantity can be estimated from below by using the Cauchy-Schwarz inequality, which states that for two vectors u, v in a Hilbert space the inequality $\|u\|^2 \|v\|^2 \geq |\langle u|v\rangle|^2$ holds true. Therefore,

$$\sqrt{\langle \hat{P}_{\mathrm{CM}} \rangle \langle \hat{R}_{\mathrm{CM}} \rangle} \geq \frac{1}{2} \left(\left| \langle \Psi_{\mathrm{gs}} | \hat{\vec{P}}_{\mathrm{CM}} \hat{\vec{R}}_{\mathrm{CM}} | \Psi_{\mathrm{gs}} \rangle \right| + \left| \langle \Psi_{\mathrm{gs}} | \hat{\vec{R}}_{\mathrm{CM}} \hat{\vec{P}}_{\mathrm{CM}} | \Psi_{\mathrm{gs}} \rangle \right| \right) \tag{B.3}$$

By application of the triangle inequality the right hand side in the inequality above we can be estimated from below as

$$\sqrt{\langle \hat{P}_{\mathrm{CM}} \rangle \langle \hat{R}_{\mathrm{CM}} \rangle} \geq \frac{1}{2} \left(\left| \langle \Psi_{\mathrm{gs}} | \hat{\vec{P}}_{\mathrm{CM}} \hat{\vec{R}}_{\mathrm{CM}} | \Psi_{\mathrm{gs}} \rangle - \langle \Psi_{\mathrm{gs}} | \hat{\vec{R}}_{\mathrm{CM}} \hat{\vec{P}}_{\mathrm{CM}} | \Psi_{\mathrm{gs}} \rangle \right| \right). \tag{B.4}$$

The right-hand side is clearly the expectation value of the commutator of the CM position and momentum operator, and thus by the canonical commutation rules can be replaced by $3i\hbar$.[1] Therefore, I get that

$$\sqrt{\langle \hat{P}_{\mathrm{CM}} \rangle \langle \hat{R}_{\mathrm{CM}} \rangle} \geq \frac{3\hbar}{2}. \tag{B.5}$$

Inserting this is in equation B.1 it is clear that $\xi_{\mathrm{CM}} \geq 0$. ■

B.2 Proof that $\mathrm{tr}\{\hat{\rho}^2\} = 1$ only for pure quantum states

A quantum system that is a subsystem of a larger one, can either be in a pure quantum state or a mixed quantum state [33]. If the system is in a pure quantum state, $|\Psi\rangle$, the corresponding density matrix can be written as $\hat{\rho} = |\Psi\rangle \langle\Psi|$. If, on the other hand, the system is in a mixed state it can be in any of N ortho-normal states $|\Psi_i\rangle$ with probability $p_i > 0$ for $i = 1, \cdots, N$, such that $\sum_{i=1}^{N} p_i = 1$. The corresponding density matrix for a mixed quantum state is $\hat{\rho} = \sum_{i=1}^{N} p_i |\Psi_i\rangle \langle\Psi_i|$.

From this it is obvious that $\mathrm{tr}\{\hat{\rho}\} = 1$ for both mixed and pure quantum states. However, in this section I intend to prove that $\mathrm{tr}\{\hat{\rho}^2\} < 1$ for mixed quantum states and $\mathrm{tr}\{\hat{\rho}\} = 1$ for pure quantum states.

I will start with the pure case. The square of the density matrix is

$$\hat{\rho}^2 = |\Psi\rangle \langle\Psi|\Psi\rangle \langle\Psi| = |\Psi\rangle \langle\Psi| = \hat{\rho}. \tag{B.6}$$

Since the trace of the density matrix is one, the trace of the square of the density matrix must also be one.

For mixed quantum states, the square of the density matrix is

$$\hat{\rho}^2 = \hat{\rho}\hat{\rho} = \sum_{i=1}^{N} p_i^2 |\Psi_i\rangle \langle\Psi_i|, \tag{B.7}$$

Taking the trace of this we get that

$$\mathrm{tr}\left\{\hat{\rho}^2\right\} = \sum_{i=1}^{N} p_i^2. \tag{B.8}$$

[1] The three comes from the fact that I am working in three dimensions.

I complete the square and get that

$$\mathrm{tr}\Big\{\hat{\rho}^2\Big\} = \left(\sum_{i=1}^{N} p_i\right)^2 - 2\sum_{i=1}^{N-1}\sum_{j=i+1}^{N} p_i p_j. \tag{B.9}$$

The first term is 1 since it is the trace of the density matrix. The second term

$$2\sum_{i=1}^{N-1}\sum_{j=i+1}^{N} p_i p_j > 0, \tag{B.10}$$

since $p_i p_j > 0$ for all i and j and therefore we have that

$$\mathrm{tr}\Big\{\hat{\rho}^2\Big\} = 1 - \underbrace{2\sum_{i=1}^{N-1}\sum_{j=i+1}^{N} p_i p_j}_{>0} < 1. \tag{B.11}$$

From this it is clear that $\mathrm{tr}\{\hat{\rho}^2\} = 1$ if and only if the system is in a pure quantum state. ■